JOC Article

Photochemical C^2-C^6 Cyclization of Enyne−Allenes: Detection of a Fulvene Triplet Diradical in the Laser Flash Photolysis

Götz Bucher,*[,†,‡] Atul A. Mahajan,[§] and Michael Schmittel*[,§]

Lehrstuhl für Organische Chemie II, Ruhr-Universität Bochum, Universitätsstrasse 150, D-44801 Bochum, Germany, and Organische Chemie I, FB 8 (Chemie-Biologie), Universität Siegen, Adolf-Reichwein-Strasse, D-57068 Siegen, Germany

goebu@chem.gla.ac.uk; schmittel@chemie.uni-siegen.de

Received July 30, 2008

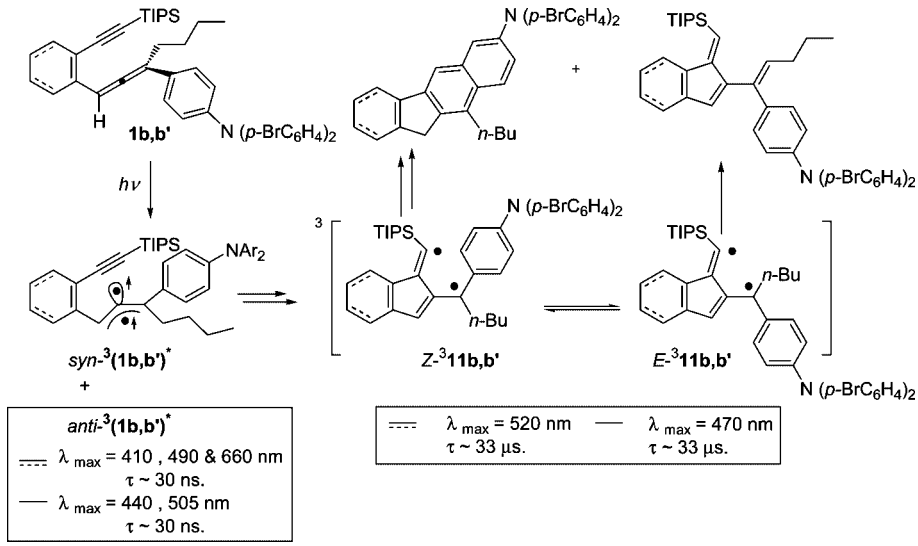

A series of enyne−allenes, with and without benzannulation at the ene moiety and equipped with aromatic and carbonyl groups as internal triplet sensitizer units at the allene terminus, was synthesized. Both sets, the cyclohexenyne−allenes and benzenyne−allenes, underwent thermal C^2-C^6 cyclization exclusively to formal ene products. In contrast, the photochemical C^2-C^6 cyclization of enyne−allenes provided formal Diels−Alder and/or ene products, with higher yields for the benzannulated systems. A raise of the temperature in the photochemical cyclization of enyne−allene **1b′** led to increasing amounts of the ene product in relation to that of the formal Diels−Alder product. Laser flash photolysis at 266 and 355 nm as well as triplet quenching studies for **1b,b′** indicated that the C^2-C^6 cyclization proceeds via the triplet manifold. On the basis of a density functional theory (DFT) study, a short-lived transient ($\tau = 30$ ns) was assigned as a triplet allene, while a long-lived transient ($\tau = 33$ μs) insensitive to oxygen was assigned as fulvene triplet diradical. An elucidation of the reaction mechanism using extensive DFT computations allowed rationalization of the experimental product ratio and its temperature dependence.

Introduction

Thermal cycloaromatizations of enediynes (Bergman cyclization)[1] and enyne−allenes/enyne−cumulenes (Myers−Saito cyclization)[2] to highly reactive diradicals characterize the modus operandi of the so-called natural enediyne antitumor antibiotics, which through the abstraction of hydrogen atoms from DNA ultimately ignite cell death.[3] As a consequence, the design of new trigger protocols for the activation of simple model compounds has become an active field of research. Among the various trigger mechanisms, the photochemical activation of enediynes along the Bergman pathway[4] has lately received great

† Ruhr-Universität Bochum.
‡ Current address: WestCHEM Research School, Department of Chemistry, University of Glasgow, Joseph-Black-Building, University Avenue, Glasgow G12 8QQ, United Kingdom.
§ Universität Siegen.

10.1021/jo801689w CCC: $40.75 © 2008 American Chemical Society
Published on Web 10/15/2008

SCHEME 1. Thermal and Photochemical Myers−Saito (C^2-C^7) and C^2-C^6 Cyclizations of Enyne−Allenes

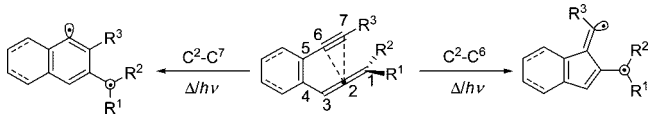

interest due to its obvious potential for photodynamic therapy (PDT).[5] In contrast, despite a first report on the photochemical Myers−Saito and C^2-C^6 cyclization in 2005 (Scheme 1),[6] the photochemical activation of enyne−allenes/enyne−cumulenes is still a terra incognita.

Our original study on the photochemical Myers−Saito and C^2-C^6 cyclization of enyne−allenes led to cyclohexenyne allenes as model compounds,[6] as theoretical investigations by Engels et al.[7] had suggested a high vertical excitation $T_1(S_0)$ energy for a benzannulated enyne−allene (101 kcal mol^{-1}) and a much lower one for (*Z*)-1,2,4-heptatrien-6-yne (59 kcal mol^{-1}).[8] By utilizing proper internal triplet sensitizer units at the allene terminus, we were able to ignite for the first time photochemical cyclizations of cyclohexenyne−allenes.[6] Parallel first laser flash photolysis results on the photochemical C^2-C^6 cyclization pointed to the occurrence of two intermediates. As the long-lived intermediate ($\tau = 33\ \mu s$) did not react with $^3O_2$, *n*-Bu_3SnH, and 1,4-cyclohexadiene, it was assigned to the singlet fulvenyl diradical.[6] However, it was difficult to reconcile such a long lifetime with the low barriers computed for the possible follow-up reactions.[9] Hence, an extensive study on the identity of the observable intermediates and on the details of the reaction course seemed to be warranted.

Encouraged by the successful implementation of the photochemical pathway and the wide knowledge about the effect of benzannulation,[10] regioselectivity,[11] and aromaticity[12] on the thermal Myers−Saito and C^2-C^6 cyclization, we decided to enlarge our original set of compounds to study the reaction course thoroughly by laser flash photolysis and to clarify the reaction course through extensive DFT computations. The present combination of laser flash photolysis (LFP) and DFT calculations provides a comprehensive picture of the mechanism of the photochemical C^2-C^6 cyclization.

CHART 1. Model Compounds 1a,a′−1c,c′

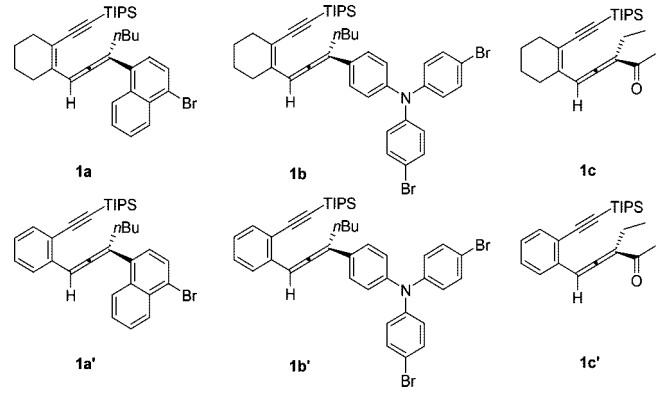

For the present investigations, we chose six enyne−allenes with and without benzannulation at the ene moiety (Chart 1) to elucidate whether photochemical cyclization would become difficult with benzannulated representatives as predicted by Engels.[7] The TIPS group at the alkyne is important to avoid thermal reactions during photolysis.[13] While parts of the results on the cyclohexenyne−allenes **1a**−**c** have been reported in our communication,[6] all results concerning the benzannulated enyne−allenes **1a′**−**c′** are new.

Results and Discussion

Synthesis of Enyne−Allenes. Sonogashira coupling of **2**[14] and **2′** with triisopropylsilyl acetylene furnished aldehydes **3** and **3′** in good yield.[15] Addition of BrMgC≡C−*n*-Bu (prepared from the reaction of EtMgBr with 1-hexyne) to **3**,**3′**, provided the corresponding propargyl alcohols **4**,**4′** in moderate yields[16] that were subsequently subjected to acetylation using acetic anhydride and DMAP in dry dichloromethane at room temperature.[17] Propargyl acetates **5**,**5′** were further reacted with ArZnCl in the presence of $Pd(PPh_3)_4$ to afford the desired enyne−allenes **1a**,**a′** and **1b**,**b′** (Scheme 2) in moderate yields.[18] Enyne−allenes **1c**,**c′** were obtained by another route as shown in Scheme 3.

Reaction of enyne−aldehyde **3** with PPh_3, zinc, and carbon tetrabromide in dry dichloromethane at room temperature afforded the dienyne **6**, which was further treated with *n*-butyllithium (2.5 M in hexane) to afford enediyne **7**.[19] The desired enyne−allene **1c** was obtained from enediyne **7** after a deprotonation using LDA and subsequent treatment with 2-bromo-3-pentanone at −78 °C. After an aqueous workup and

(1) (a) Bergman, R. G.; Jones, R. R. *J. Am. Chem. Soc.* **1972**, *94*, 660–661. (b) Bergman, R. G. *Acc. Chem. Res.* **1973**, *6*, 25–31.
(2) (a) Myers, A. G.; Kuo, E. Y.; Finney, N. S. *J. Am. Chem. Soc.* **1989**, *111*, 8057–8059. (b) Nagata, R.; Yamanaka, H.; Okazaki, E.; Saito, I. *Tetrahedron Lett.* **1989**, *30*, 4995–4998.
(3) (a) Nicolaou, K. C.; Dai, W.-M. *Angew. Chem., Int. Ed. Engl.* **1991**, *30*, 1387–1416. (b) Borders, D. B.; Doyle, T. W. *Enediyne Antibiotics as Antitumor Agents*; Marcel Dekker: New York, 1995.
(4) (a) Turro, N. J.; Evenzahav, A.; Nicolaou, K. C. *Tetrahedron Lett.* **1994**, *35*, 8089–8092. (b) Evenzahav, A.; Turro, N. J. *J. Am. Chem. Soc.* **1998**, *120*, 1835–1841. (c) Funk, R. L.; Young, E. R. R.; Williams, R. M.; Flanagan, M. F.; Cecil, T. L. *J. Am. Chem. Soc.* **1996**, *118*, 3291–3292. (d) Kaneko, T.; Takahashi, M.; Hirama, M. *Angew. Chem., Int. Ed.* **1999**, *38*, 1267–1268. (e) Choy, N.; Blanco, G.; Wen, J.; Krishan, A.; Russell, K. C. *Org. Lett.* **2000**, *2*, 3761–3764. (f) Clark, A. E.; Davidson, E. R.; Zaleski, J. M. *J. Am. Chem. Soc.* **2001**, *123*, 2650–2657. (g) Chandra, T.; Kraft, B. J.; Huffman, J. C.; Zaleski, J. M. *Inorg. Chem.* **2003**, *42*, 5158–5172. (h) Benites, P. J.; Holmberg, R. C.; Rawat, D. S.; Kraft, B. J.; Klein, L. J.; Peters, D. G.; Thorp, H. H.; Zaleski, J. M. *J. Am. Chem. Soc.* **2003**, *125*, 6434–6446.
(5) (a) Boyle, R. W.; Dolphin, D. *Photochem. Photobiol.* **1996**, *64*, 469–485. (b) Mody, T. M., Sessler, J. L., Eds. *Supramolecular Materials and Technologies*; Wiley: Chichester, U.K., 1999; Vol. 4. (c) Ali, H.; van Lier, J. E. *Chem. Rev.* **1999**, *99*, 2379–2450. (d) Bonnett, R.; Martinez, G. *Tetrahedron* **2001**, *57*, 9513–9547. (e) Ackroyd, R.; Kelty, C.; Brown, N.; Reed, M. *Photochem. Photobiol.* **2001**, *74*, 656–669.
(6) Schmittel, M.; Mahajan, A. A.; Bucher, G. *J. Am. Chem. Soc.* **2005**, *127*, 5324–5325.
(7) Spöler, C.; Engels, B. *Chem.—Eur. J.* **2003**, *9*, 4670–4677.
(8) Private communication by Prof. B. Engels.
(9) (a) Musch, P. W.; Engels, B. *J. Am. Chem. Soc.* **2001**, *123*, 5557–5562. (b) Bekele, T.; Christian, C. F.; Lipton, M. A.; Singleton, D. A. *J. Am. Chem. Soc.* **2005**, *127*, 9216–9223. (c) Schmittel, M.; Vavilala, C.; Jaquet, R. *Angew. Chem., Int. Ed.* **2007**, *46*, 6911–6914.
(10) Wenthold, P. G.; Lipton, M. A. *J. Am. Chem. Soc.* **2000**, *122*, 9265–9270.
(11) Musch, P. W.; Remenyi, C.; Helten, H.; Engels, B. *J. Am. Chem. Soc.* **2002**, *124*, 1823–1828.
(12) Stahl, F.; Moran, D.; Schleyer, P. v. R.; Prall, M.; Schreiner, P. R. *J. Org. Chem.* **2002**, *67*, 1453–1461.
(13) Schmittel, M.; Strittmatter, M.; Mahajan, A. A.; Vavilala, C.; Cinar, M. E.; Maywald, M. *ARKIVOC* **2007**, 66–84 (Part viii).
(14) For the synthesis of compound **2** see: (a) Arnold, Z.; Holy, A. *Collect. Czech. Chem. Commun.* **1961**, *26*, 3059–3073. (b) Salem, B.; Delort, E.; Klotz, T.; Suffert, J. *Org. Lett.* **2003**, *5*, 2307–2310.
(15) Schmittel, M.; Steffen, J.-P.; Maywald, M.; Engels, B.; Helten, H.; Musch, P. *J. Chem. Soc., Perkin Trans. 2* **2001**, 1331–1339.
(16) Schmittel, M.; Strittmatter, M.; Schenk, W. A.; Hagel, M. *Z. Naturforsch. B* **1998**, *53*, 1015–1020.
(17) Fleming, I.; Terrett, N. K. *J. Organomet. Chem.* **1984**, *264*, 99–118.
(18) Elsevier, C. J.; Stehouwer, P. M.; Westmijze, H.; Vermeer, P. *J. Org. Chem.* **1983**, *48*, 1103–1105. For the synthesis of **1a**, see: ref 13.
(19) Herndon, J.; Wang, H. *J. Org. Chem.* **1998**, *63*, 4562–4563.

SCHEME 2. Synthesis of Enyne−Allenes 1a,a′ and 1b,b′[a]

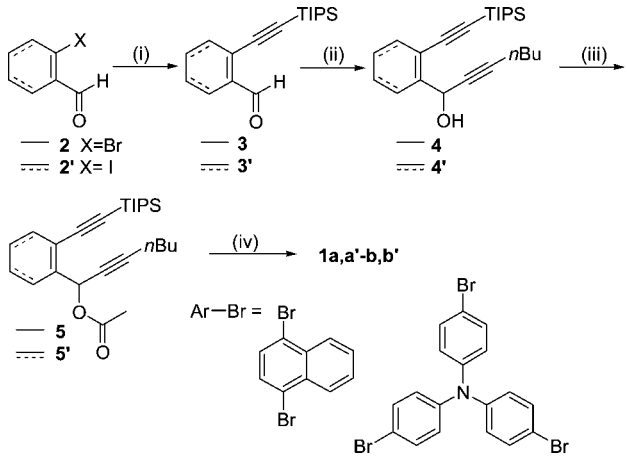

[a] Reagents and conditions: (i) H−C≡C−TIPS, $Pd(PPh_3)_2Cl_2$, CuI, Et_3N, rt, 16 h, **3**: 94%, **3′**: 92%; (ii) EtMgBr, H−C≡C−*n*Bu, THF, rt, **4**: 78%, **4′**: 88%; (iii) Ac_2O; DMAP, Et_3N, rt, 16 h, **5**: 80%, **5′**: 98%; (iv) Ar−Br, *n*BuLi/ $ZnCl_2$ (1 M in diethyl ether)/ $Pd(PPh_3)_4$, −60 °C to rt, 16 h, **1a**: 40%, **1a′**: 30%, **1b**: 62%, **1b′**: 48%.

SCHEME 3. Synthesis of Enyne−Allenes 1c,c′[a]

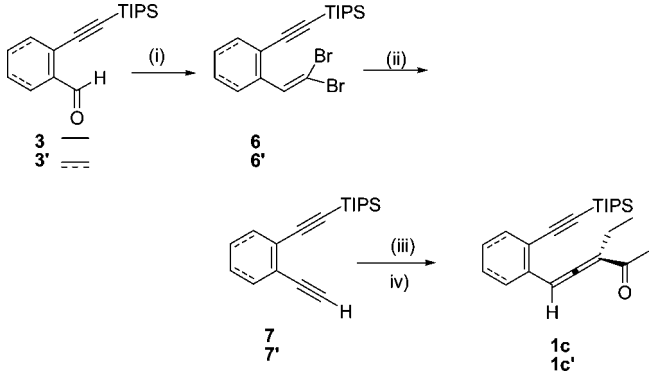

[a] Reagents and conditions: (i) PPh_3, Zn, CBr_4, DCM, 40 h, rt, **6**: 86%, **6′**: 92%; (ii) *n*-BuLi, THF, −78 °C to rt, 3 h, **7**: 75%, **7′**: 71%; (iii) LDA, HMPA, 2-bromo-3-pentanone, −78 °C, THF; (iv) SiO_2, **1c**: 42%, **1c′**: 32%.

column chromatography, enyne−allene **1c** was received in 42% yield (Scheme 3). Mechanistic aspects of this tranformation have been addressed earlier.[20] The benzannulated enyne−allene **1c′** was prepared analogously.

Thermal Cyclization. In accord with the thermolysis of other enyne−allenes containing bulky groups at the alkyne terminus,[21a−c] the thermal cyclization of cyclohexenyne−allenes **1a−c** and benzenyne−allenes **1a′-c′** in dry toluene at 110 °C furnished exclusively the formal ene products **8a−c** and **8a′−c′** in mostly good yields (Table 1, Scheme 4). In general, thermal product formation from the benzannulated enyne−allenes was distinctly cleaner. Only in the thermolysis of enyne−allene **1b′** a trace amount (<1%) of the formal Diels−Alder product **10b′** was formed.[21c]

The thermal reactivity of enyne−allenes **1a−c** and **1a′−c′** was evaluated by measuring the temperature T_{onset} of the exothermic signal in differential scanning calorimetry (DSC) experiments.

TABLE 1. T_{onset} from DSC Measurements of the Thermal Cyclization of Enyne−Allenes 1a−c and 1a′−c′ and the Yield of Their Cyclization Products

enyne−allene	T_{onset} (°C)			% yield
cyclohexenyne−allenes	**1a**, 152	**1b**, 143	**1c**, 151	**8a**, 67; **8b**, 68; **8c**, 42
benzannulated enyne−allenes	**1a′**, 128	**1b′**, 108	**1c′**, 126	**8a′**, 91; **8b′**, 83; **8c′**, 80

SCHEME 4. Thermal Cyclization of Enyne−allenes 1a,a′−c,c′

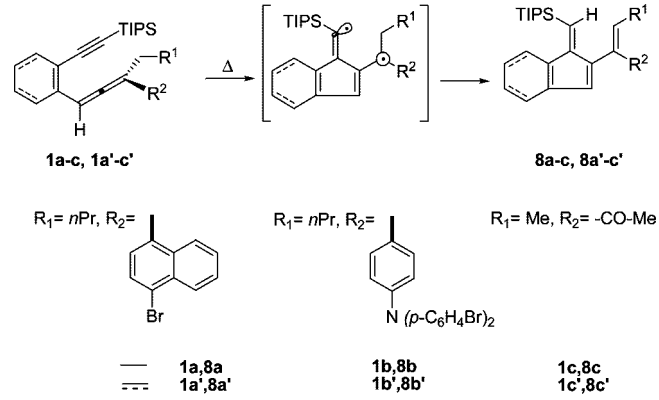

The DSC experiments showed T_{onset} for the cyclization of cyclohex-enyne−allenes to be reproducibly higher than for its benzannulated analogs (Table 1). For example, the temperature for the thermal cyclization of **1b′** is lower by 35 °C than that of **1b**, thus emphasizing that benzannulation decreases the activation barrier in agreement with the earlier theoretical findings by Wenthold and Lipton[10] and Engels.[22]

Photochemical Cyclization of Enyne−allenes 1a−c and 1a′−c′. Photolysis of enyne−allene **1a′** in dry degassed toluene (1−2 mM; details see Table 2 and Scheme 5) in the presence of 1,4-cyclohexadiene (1,4-CHD; 100-fold excess) provided the formal Diels−Alder product **9a′** (8%) as the only isolable low molecular weight compound. The ^1H NMR spectrum showed a characteristic singlet at 4.29 ppm for the CH_2 unit of the fluorene subunit and a benzylic triplet at 2.73 ppm of the $-CH_2Pr$ unit ($^3J = 7.9$ Hz). The analogous irradiation of **1a** did not lead to any isolable product.[6] Irradiation of enyne−allene **1b′** (1.27 mM) in dry degassed toluene furnished a mixture of two isomeric ene products[23] **8b′** and (*E*)-**8b′** in 32% yield along with 18% of the formal Diels−Alder product **10b′**. In contrast, the photochemical cyclization of cyclohexenyne−allene **1b** provided ene product **8b** and formal Diels−Alder product **10b** in a 1:1 ratio.[6] In both **10b** and **10b′**, the TIPS group was lost, contrary to the situation in **9a′**. Recent experimental and computational studies showed that the desilylation in the formal Diels−Alder product takes place after a silyl shift in the primary Diels−Alder adduct.[24]

Under analogous conditions, the photolysis of enyne−allene **1c′** furnished four isomers of the C^2-C^6 product in moderate total yield (51%) (Scheme 6 and Table 2) that were separated

(20) Schmittel, M.; Strittmatter, M. *Tetrahedron* **1998**, *54*, 13751–13760.
(21) (a) Schmittel, M.; Strittmatter, M.; Kiau, S. *Tetrahedron Lett.* **1995**, *36*, 4975–4978. (b) Schmittel, M.; Kiau, S.; Strittmatter, M. *Angew. Chem., Int. Ed.* **1996**, *35*, 1843–1845. (c) Schmittel, M.; Keller, M.; Kiau, S.; Strittmatter, M. *Chem.−Eur. J.* **1997**, *3*, 807–816. (d) Schmittel, M.; Kiau, S.; Siebert, T.; Strittmatter, M. *Tetrahedron Lett.* **1996**, *37*, 7691–7694. (e) Engels, B.; Lennartz, C.; Hanrath, M.; Schmittel, M.; Strittmatter, M. *Angew. Chem., Int. Ed.* **1998**, *37*, 1960–1963.
(22) Musch, P. W.; Engels, B. *J. Am. Chem. Soc.* **2001**, *123*, 5557–5562.
(23) *E*-**8b′** arises most likely from the irradiation of the photolabile C^2-C^6 product **8b′**. This was tested by independent irradiation of **8b′** (isolated from the thermal reaction).
(24) Schmittel, M.; Mahajan, A. A.; Bucher, G.; Bats, J. W. *J. Org. Chem.* **2007**, *72*, 2166–2173.

TABLE 2. Yields of Photochemical C²−C⁶ Product after Irradiation at 300 nm

compd (conc, mM)	solvent (irradiation time, h)	λ_{max}/nm (in hexane)	ene product (yield, %)[d]	DA product (yield, %)[d]
1a (1.78)[a]	toluene + 1,4-CHD[b] (6)	280, 297		
1a′ (1.14)	toluene + 1,4-CHD[b] (1)	277, 283, 293		8
1b (1.36)[a]	toluene + 1,4-CHD[b] (6)	281, 318	15	15
1b′ (1.27)	toluene + 1,4-CHD[b] (6)	266, 318	32	18
1c (5.28)[a]	*n*-hexane + 1,4-CHD[c] (14)	279, 290 (sh)	32[e]	
1c′ (1.69)	*n*-hexane + 1,4-CHD[b] (36)	236, 272, 282 (sh)	51	

[a] Reference 6. [b] In the presence of 1,4-CHD (100-fold excess); DA- formal Diels−Alder. [c] 2:1 mixture. [d] Isolated yield. [e] Isolated yield: **8c′** (29%), (*E*)-**8c′** (16%), **8c″** (6%).

SCHEME 5. Photochemical Cyclization of Enyne−Allenes 1a′, 1b, and 1b′

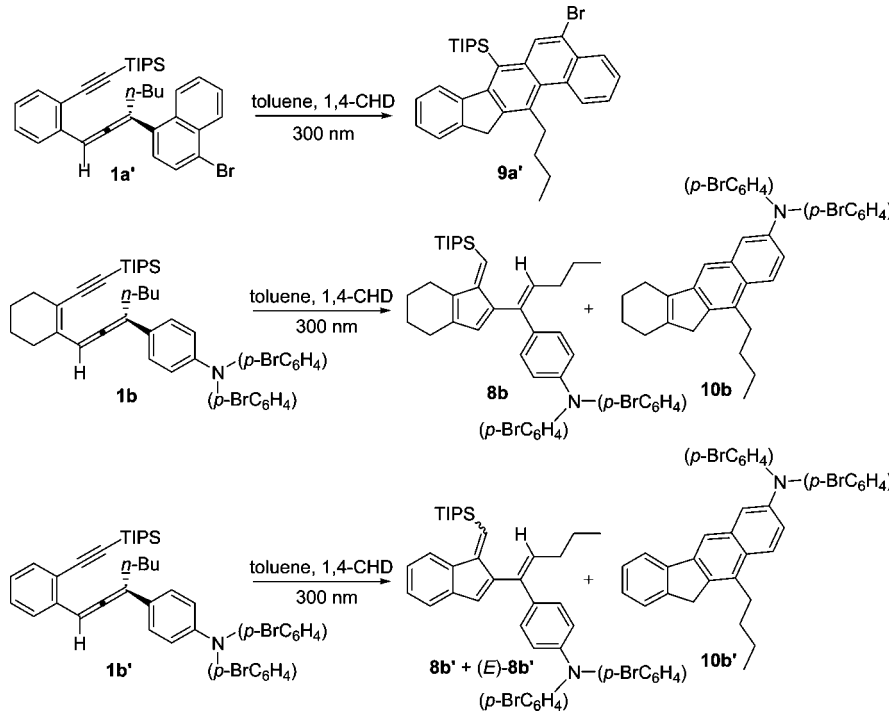

SCHEME 6. Photochemical Cyclization of Enyne−Allenes 1c and 1c′

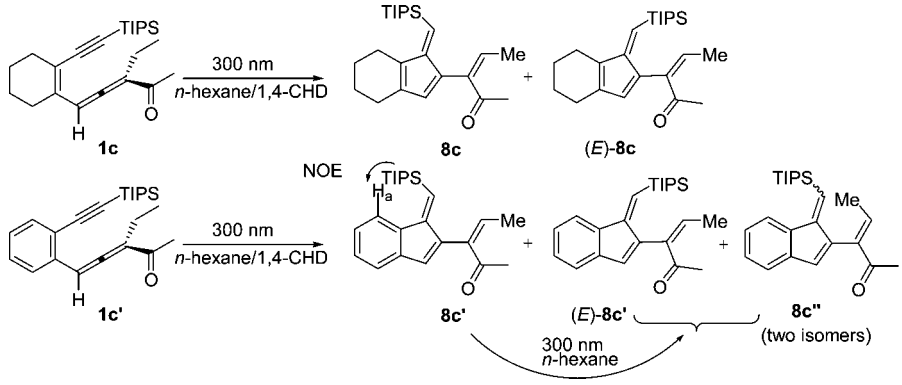

into three fractions representing **8c′**, (*E*)-**8c′**, and **8c″** (the latter as a mixture of two isomers). Compound **8c′** was the main product with 29% yield. Independent irradiation of **8c′**, readily produced from thermal cyclization of **1c′**, at 300 nm in dry degassed *n*-hexane furnished the photoproducts (*E*)-**8c′** and **8c″**. This suggests that products (*E*)-**8c′** and **8c″** emerging during photolysis of **1c′** equally arose in a follow-up photo process from the photolabile product **8c′**. The geometry at the *exo*-methylene double bond of **8c′** was clearly assigned on the basis of NOESY spectra. The aromatic proton H_a in **8c′** showed a diagnostic NOE signal with the TIPS group; consequently, compound **8c′** has a (*Z*)-geometry at the fulvenyl *exo*-double bond. While the configurations at all stereogenic double bonds in (*E*)-**8c′** could be clarified by NOE investigations, this was not possible for the isomeric mixture of **8c″**.[25]

Since the laser flash photolysis experiments (vide infra) pointed toward a wavelength dependence of the reaction mechanism, we studied also the preparative 350-nm photolysis of enyne−allene **1b′** in dry toluene in the presence of 1,4-

(25) Despite the use of g-NOESY and g-ROESY NMR techniques the precise geometry at the *exo*-methylene double bond of C²−C⁶ product (**9d-1**) could not be clarified.

TABLE 3. Triplet-Quenching Reaction of Enyne−Allenes (1 mM)

compd	triplet quencher	irradiation time (h)	C^2-C^6 product (yield, %)
1b	1,4-diphenylbutadiene[a]	7	0
1b	$^3O_2$[b]	7	0
1b′	$^3O_2$[b]	3	12 (ene)

[a] 15 equiv of 1,4-diphenyl-1,3-butadiene was used. [b] $^3O_2$ was continuously bubbled through the reaction mixture.

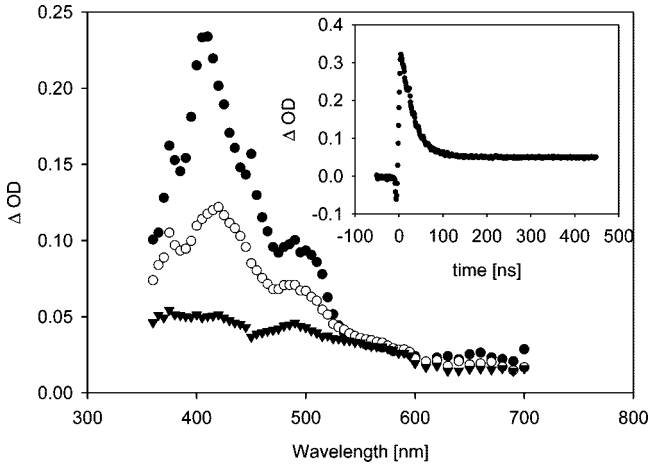

FIGURE 1. Transient spectra, observed during different time intervals after LFP (355 nm) of enyne−allene **1b′** in degassed cyclohexane. Black circles: 8 ns after LFP, light circles: 43 ns after LFP, black triangles: 380 ns after LFP. Inset: transient trace, monitored at $\lambda = 410$ nm.

cyclohexadiene. The reaction furnished both ene (38%, two isomers) and DA (16%) products, an outcome very similar to that after irradiation at 300 nm. Additionally, two side products were isolated whose ^{1}H NMR and ESI-MS unfortunately did not allow for a final structural assignment.

Mechanistic Experiments. When the photochemical cyclization of enyne−allene **1b** was carried out in the presence of triplet quenchers such as 1,4-diphenyl-1,3-butadiene (42 kcal mol^{-1})[26] or $^3O_2$, the cyclization of **1b** was completely suppressed. Along the same line, the photochemical cyclization of enyne−allene **1b′** in the presence of $^3O_2$ furnished a lower yield of the ene product 12% (Table 3). Hence, the triplet quenching studies strongly suggest that the photochemical C^2-C^6 cyclization proceeds along the triplet manifold.

The effect of temperature (20−60 °C) on the photochemical C^2-C^6 cyclization was studied with enyne−allene **1b′**. With cyclohexenyne−allene **1b**, the same investigation was not feasible due to its thermal instability at 40−60 °C. Photolysis (300 nm) of **1b′** at 20 °C afforded ene and Diels−Alder products in 32% and 18% yield. The data (Table 4) show that with increasing temperature the yield of **8b′** roughly remained constant, while the yield of the formal DA product **10b′** declined drastically from 18% (20 °C) to 8% (40 °C) and finally <2% (60 °C). While the decreasing yield of the Diels−Alder product might imply that in compensation the yield of the ene product should augment with increasing temperature, we did not observe such trend. This is possibly due to an instability of the ene product at 40−60 °C under photochemical conditions. Although a final analysis has to await the outcome of the laser photolysis study (vide infra), the preparative results suggest that at higher temperature two rotameric fulvenyl diradicals may interconvert (Scheme 7).

TABLE 4. Photoreactivity of Enyne−Allene 1b′ at Different Temperatures

solvent	irradiation time (h)	T/°C	ene product[a] **8b′**	Diels−Alder product[a] **10b′** (%)
toluene	6	20 ± 1	32	18
toluene	3	40 ± 1	27	8
toluene	1.5	60 ± 1	27	trace

[a] Isolated yield.

Laser Flash Photolysis of 1b. In order to gain information on the reaction mechanism and to identify possible intermediates in photochemical enyne−allene C^2-C^6 cyclizations, we have performed a LFP (laser flash photolysis) study of **1b** and **1b′**. Results obtained with enyne−allene **1b** had previously been published in preliminary form;[6] they will be presented in greater detail here. As reported earlier, LFP of **1b** ($\lambda_{exc} = 355$ nm, cyclohexane solution, 1 atm of Ar) resulted in the observation of transient phenomena on both short (ns) and longer (μs) time scales. On the short time scale, a transient ($\lambda_{max} = 440$ and 505 nm, $\tau = 30$ ns; see Figure S1 in the Supporting Information and also Figure 3) was observed that was quenched by $^3O_2$ ($k_q = (1.8 \pm 0.3) \times 10^9$ l mol^{-1} s^{-1}; see Figure S2 in the Supporting Information). It is not quenched by 1,3-cyclohexadiene. Based on its high reactivity toward triplet oxygen, we had previously assigned this short-lived transient to **^{3}1b**, the first triplet excited-state of **1b**.[6]

On a longer time scale, a second transient was observed ($\lambda_{max} = 480$ nm, $\tau = (33 \pm 5)$ μs, see Figure 5). This transient was not measurably quenched by 1,4-cyclohexadiene (up to 0.5% by volume) or tri-*n*-butylstannane. Purging the solution with oxygen resulted in a decrease in transient intensity, while its lifetime remained constant. A plot of the inverse transient intensity ($1/\Delta$OD) vs. oxygen concentration (SV plot: Stern−Volmer plot) was rather noisy because of poor signal-to-noise ratio due to the small transient intensity and the use of a baseline compensator. Nevertheless, a linear correlation was observed, with $k_q \tau = 17550/169 = 104$. With $k_q = 1.8 \times 10^9$ L mol^{-1} s^{-1}, the lifetime of the precursor transient to the long-lived transient is obtained as $\tau = 58$ ns. Given the rather noisy SV plot, this is in reasonable agreement with the directly measured value $\tau = 30$ ns for the short-lived transient assigned to **^{3}1b**. This observation suggests that the short-lived transient is a direct precursor to the long-lived transient.[6] (Figure S3 shows transient spectra in the microsecond regime observed upon LFP at 355 nm of **1b**, Figure S4 displays a transient difference spectrum, and Figure S5 shows the Stern−Volmer plot; see the Supporting Information).

Previously, we had assigned the 480 nm transient to a singlet diradical formed from **^{3}1b** by C^2-C^6 cyclization.[6] This preliminary assignment had been based on the lack of direct reactivity of the 480 nm - transient toward oxygen. However, calculations now indicate that the ground-state of silyl-functionalized fulvene diyls possibly is a triplet; see below.

LFP of **1b** in cyclohexane at $\lambda_{exc} = 266$ nm employing the fourth harmonic of a Nd:YAG laser gave results that were similar to the results obtained using $\lambda_{exc} = 355$ nm.

Laser Flash Photolysis of 1b′. As in the case of cyclohexenyne−allene **1b**, two transients were observed for the benzannulated enyne−allene **1b′** using $\lambda_{exc} = 355$ nm. The first

(26) *Handbook of photochemistry*, 2nd ed.; Murov, S. L., Carmichael, I., Hug, G. L., Eds.; Marcel Dekker/CRC Press: Boca Raton, 1993.

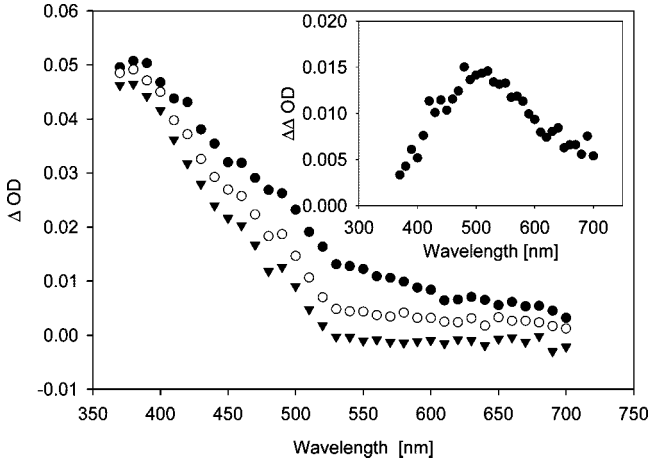

FIGURE 2. Transient spectra, observed during different time intervals after LFP (355 nm) of enyne−allene **1b′** in degassed cyclohexane. Black circles: 7.9 μs after LFP, light circles: 34 μs after LFP, black triangles: 150 μs after LFP. Inset: transient difference spectrum (7.9 μs minus 150 μs).

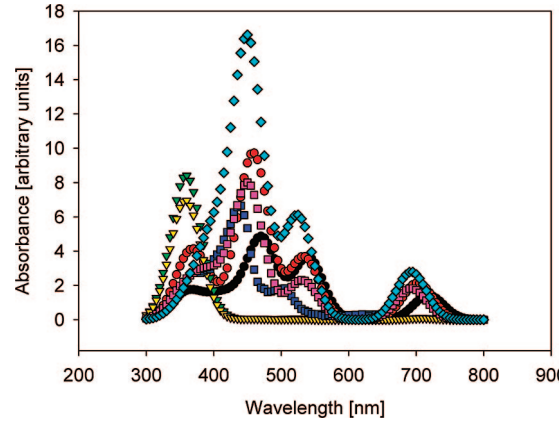

FIGURE 3. Comparison of calculated UV/vis spectra (TD-UB3LYP/6-31+G*//UB3LYP/6-31G*) of the four isomeric triplet states of **1B** with the experimental transient spectrum observed 16 ns after LFP (355 nm) of **1b** in cyclohexane (cf. Figure S1, Supporting Information). Red: *syn-E*-**1B**-triplet II. Black: *syn-Z*-**1B**-triplet II. Magenta: *anti-E*-**1B**-triplet II. Light blue: *anti-Z*-**1B**-triplet II. Green: *anti-lk*-**1B**-triplet I. Yellow: *anti-ul*-**1B**-triplet I. Dark blue: experimental spectrum, scaled to match the calculated spectra in intensity.

short-lived transient ($\tau \sim 30$ ns) showed maxima at $\lambda = 410$ and 490 nm along with a very weak maximum at 660 nm (Figure 1). This transient was not measurably quenched by $^3O_2$. Due to the very fast decay kinetics in the absence of oxygen, this observation places an upper limit of $k_{O2} \approx 5 \times 10^8$ L mol^{-1} s^{-1} on the oxygen-quenching reaction, while a k_{O2} smaller than this value is not ruled out. The second transient exhibited a much longer lifetime ($\tau = 33$ μs). Its absorption maximum ($\lambda_{max} =$ 520 nm) was red-shifted compared to that of the long-lived transient (λ_{max} at 470 nm) observed upon excitation of cyclohexenyne−allene **1b**. The long-lived transient also did not show any measurable direct reactivity toward $^3O_2$.

Figure 1 displays the spectrum of the short-lived transient observed upon LFP of **1b′**. Figure 2 shows a transient spectrum of the long-lived transient. Its absorption maximum is most easily discerned in the transient difference spectrum (black circles minus black triangles) as provided in the inset of Figure 2.

We also investigated the photochemistry of **1b′** in cyclohexane using the fourth harmonic of a Nd:YAG laser ($\lambda_{exc} = 266$ nm) as excitation light source. Under these conditions, two weakly absorbing transient species were observed which were different from the ones detected upon 355 nm excitation (Figures S6−S8, Supporting Information). A short-lived transient was found to have a lifetime $\tau = (60 \pm 10)$ ns with $\lambda_{max} = 415$ nm and a broad band extending to $\lambda = 700$ nm and probably beyond. (Figure S7, see the Supporting Information). The second, longer-lived transient ($\tau = (3.0 \pm 0.5)$ μs, $\lambda_{max} = 395$, 485 nm and a broad band extending beyond 650 nm, see Figure S6 in the Supporting Information) was not directly quenched by oxygen. Stern−Volmer (SV) quenching of this species by $^3O_2$, on the other hand, was observed (Figure S9, see the Supporting Information). From the SV plot, the product of lifetime and rate constant of decay of the precursor to the 395/485 nm transient was derived as $k_q * \tau = 86$. Assuming $\tau = 60$ ns, k_q follows as $k_q = 1.4 * 10^9$ L mol^{-1} s^{-1}. As this is a reasonable value for oxygen quenching of an excited-state or a reactive diradical, it appears likely that the precursor transient detected indirectly by SV-quenching in fact is the short-lived 415 nm transient also monitored directly.

The observation of two entirely different sets of transients upon 355 and 266 nm excitation of **1b′** is puzzling. If one looks at the reactivity pattern and transient spectra, it appears that the transients observed upon 266 nm excitation of **1b′** are similar to the transients observed upon LFP of **1b**. In both cases, a transient with a lifetime in the microsecond regime is observed, with spectroscopic properties that are similar (compare Figures S3 and S6; see the Supporting Information). Both **1b** and **1b′** (266 nm excitation) also yield a short-lived transient with a lifetime of the order of 30−60 ns. In both cases, this transient is quenched by oxygen, as is shown both directly and by the Stern−Volmer quenching observed. It is thus tempting to conclude that **1b′** upon 266 nm excitation, like **1b**, yields a fulvenediyl-type diradical whose formation is preceded by decay of an allene-type triplet state. What, however, would then be a possible assignment for the transients observed upon 355 nm LFP of **1b′**? We will discuss this issue later in context with the results of our calculations.

Calculations of Triplet Allenes. Energies and UV/vis Spectra. In order to come to more reliable assignments of the transient species observed in the two sets of experiments, we have employed density functional theory ((U)B3LYP/6-31G(d)) to optimize the geometries of a number of species and to predict some of their properties of interest. Calculated UV/vis spectra should prove particularly helpful in confirming or disproving an assignment. We therefore employed time-dependent DFT (TD-UB3LYP/6-31+G(d)//UB3LYP/6-31G(d)) to calculate the UV/vis spectra of the triplet excited states of a series of model compounds for transients derived from **1b** and **1b′**. In order to stay as close as possible to the experimental system, only the remote bromine atom substituents were omitted in our model system, and the *n*-butyl substituent was replaced by methyl, resulting in compounds **1B** (as model for **1b**) and **1B′** (as model for **1b′**). DFT calculations on the model precursors showed that the *syn*-conformers were higher in energy than the *anti*-conformers, as expected (Scheme 8). However, RIMP2 single-point energy calculations (based on the geometries obtained by DFT) indicated that DFT underestimates the stability of the *syn*-conformers by ca. 6 kcal mol^{-1}. At the RIMP2 level of theory, the *syn*-conformers were actually predicted to be energetically more favorable than the *anti*-conformers. This

SCHEME 7. Preliminary Summary of LFP Results of 1b and 1b′

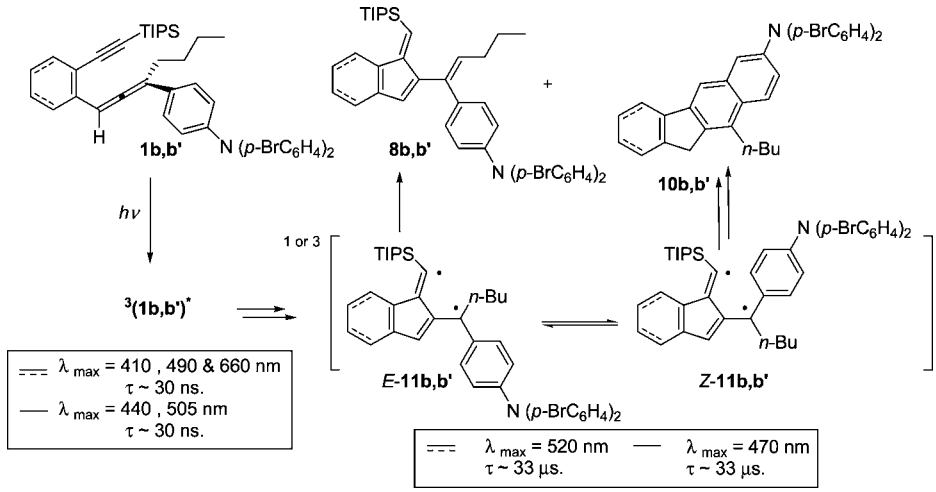

SCHEME 8. Conformers of Model Precursors 1B and 1B′; Energies in kcal mol^{-1} Relative to the *Anti* Conformers (Top (roman font): B3LYP/6-31G(d). Bottom (Italics): RIMP2/TZVP//B3LYP/6-31G(d))

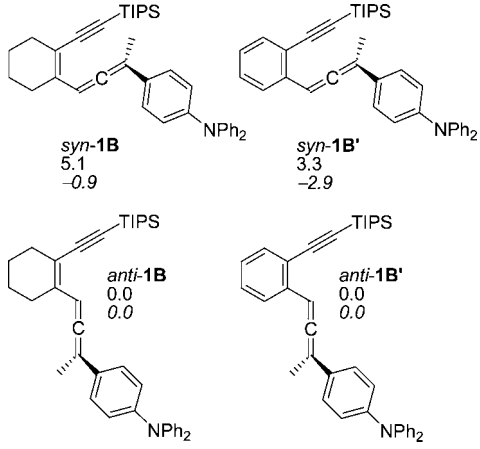

is likely due to the fact that weak long-range interactions are poorly described by DFT.

In the case of **1B**, two fundamentally different triplet excited states could be located (Scheme 9). The first of the two is of a triplet alkene-type (triplet I), with a strongly twisted double bond ($\theta = -56.9°$) in the cyclohexene moiety. Excitation to triplet I hence introduces helicity into the molecule, which combines with the axial chirality of the allene unit. Hence, *lk* and *ul* diastereomers of **1B**-triplet I should exist in both *syn*- and *anti*-conformations. According to our calculations, the triplet energy is $E_T \approx 43$ kcal mol^{-1} for all diastereomers. The second triplet excited-state located for **1B** (triplet II) is of the triplet allene-type (allyl−vinyl diradical) with a nonlinear allene moiety. Four stereoisomers of triplet II are predicted to exist, with calculated triplet energies somewhat below 40 kcal mol^{-1} (Scheme 9). Triplet energies somewhat below 40 kcal mol^{-1} are consistent with published experimental triplet energies of arylallenes, e.g., the triplet energy of tetraphenylallene[27] has been reported as $E_T = (40.2 \pm 0.7)$ kcal mol^{-1}.

The activation enthalpy for interconversion of the *syn*- and *anti*-stereoisomers of **1B** triplet II is calculated as $\Delta H^{\ddagger} = 12.3$ kcal mol^{-1} for the endothermic conversion of *anti-Z*-**1B** triplet II into *syn-Z*-**1B** triplet II. Attempts to optimize the transition states of a direct interconversion of *E*- and *Z*-isomers yielded the alkene-type triplet I isomers. While their relatively low energy may thus facilitate a direct *Z*-/*E*-equilibration of triplet excited **1B**, we note that barriers of the order of 10 kcal mol^{-1} for such a reaction are significant considering the inherently short lifetimes of the triplet states involved. Finally, we note that an optimization of triplet **1B** using the optimized geometry of singlet ground state *anti*-**1B** as starting geometry yielded the higher energy twisted alkene triplet I state of **1B** rather than the allene-type triplet II state.

In case of the benzannulated system **1B′**, no twisted alkene-type triplet states could be located, which is unsurprising considering the loss of aromaticity connected with such a structure. As in the case of **1B**, four stereoisomeric allene-type triplet states (triplet II) could be located. Again, the triplet enthalpies are consistently around 40 kcal mol^{-1} (Scheme 10). Due to the absence of accessible alkene-type triplet states, interconversion of *Z*- and *E*-stereoisomers is predicted to be a single-step reaction in this system. Because of its significant barrier an *E*-/*Z*-interconversion is unlikely to take place during the very short lifetime of triplet **1B′**. In order to test for the influence of the DFT method, additional calculations using the UBLYP method were performed here. As a result, we note that changing the functional from B3LYP to BLYP does essentially nothing to the enthalpies calculated.[28b]

Assignment of the Short-Lived Intermediates of 1b and 1b′. The calculated UV/vis spectra of six isomeric triplet states of **1B** are given in Figure 3, along with a scaled experimental spectrum (in dark blue). It is clearly seen that only the energetically lower lying allene-type triplets (triplet II, see SCHEME 9) yield a reasonable fit with the experimental spectrum, while the alkene-type triplets (triplet I) are not predicted to show any significant absorption beyond $\lambda = 440$ nm. As the calculated spectra for all stereoisomers of **1B**-triplet

(27) Brennan, C. M.; Caldwell, R. A.; Elbert, J. E.; Unett, D. J. *J. Am. Chem. Soc.* **1994**, *116*, 3460–3464.

(28) (a) Errors in calculated spectra are larger at long wavelengths (an energy difference corresponding to 20 nm wavelength difference at $\lambda = 200$ nm amounts to 100 nm wavelength difference at $\lambda = 1000$ nm). Our omission of the remote bromine atom substituents may also contribute to deviations between calculated and experimental spectra. (b) This statement also holds, if the biradicals and final products are included into the consideration. For the SP energies, see the Supporting Information. (c) Morina, V. F.; Sveshnikova, E. B. *Opt. Spectrosc.* **1973**, *34*, 359–360.

SCHEME 9. Different Triplet Excited State Isomers of Allene 1B, Calculated (UB3LYP/6-31G(d)) Triplet Enthalpies in kcal mol^{-1}, Relative to the Singlet Ground State of *anti*-1B = 0.0 kcal mol^{-1} (The Rightmost Arrow Connects *anti-ul*-1B-Triplet I and *syn-ul*-1B-Triplet I)

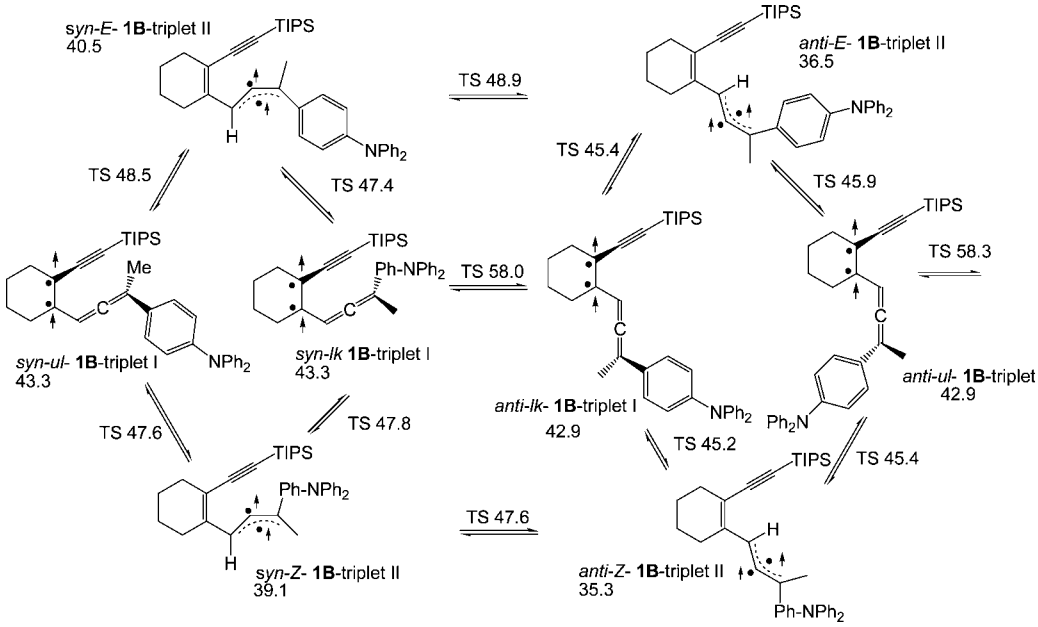

SCHEME 10. Different Allene-Type Triplet Excited State (Triplet II) Isomers of 1B′, Calculated (UB3LYP/6-31G(d)) Triplet Enthalpies in kcal mol^{-1}, Relative to the Singlet Ground State of *anti*-1B′ = 0.0 kcal mol^{-1} (Italics: Calculated at the UBLYP/6-31G(d) Level of Theory)

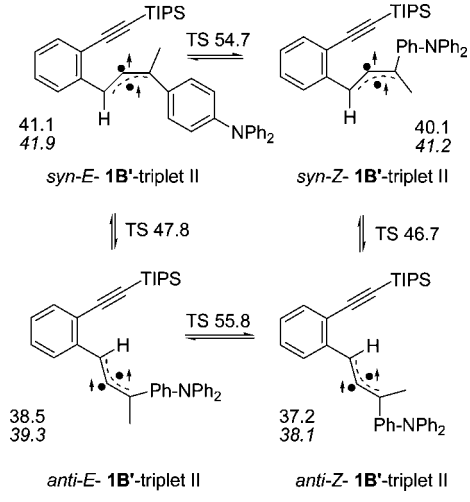

II are similar, an unambiguous assignment cannot be made based on the TD-DFT calculations.

A comparison of the calculated UV/vis spectra of the triplet II state stereoisomers of **1B′** with the experimental transient spectrum recorded upon LFP (355 nm excitation) of **1b′** shows that the agreement is reasonable with *anti*-stereoisomers (Figure 4). The blue (exptl) and yellow or green (calcd) spectra are similar in overall shape (strong absorption at $\lambda \approx 400$ nm with a weaker, not baseline-separated band at $\lambda \approx 500$ nm), only the long-wavelength near-IR absorption calculated is not observed experimentally.[28a] The *syn*-conformers, on the other hand, should show a well-separated band between $\lambda = 500$ and 600 nm, which is not observed in our experiments. Given this agreement, an assignment of the short-lived transient observed upon 355 nm LFP of **1b′** to one or two *anti*-stereoisomers of triplet-II-**1b′** seems plausible.

The agreement between the calculated triplet II spectra shown in Figure 4 and the experimental transient spectrum (Figure S6, Supporting Information) of the short-lived transient observed upon 266 nm excitation of **1b′**, on the other hand, is poor. First, the 400 nm band is calculated to be extremely intense for all triplet II state stereoisomers of **1B′**. While the short-lived transient observed upon 266 nm excitation of **1b′** does have a band in this region, it is rather weak. Second, all triplet II state stereoisomers of **1B′** are predicted to show a prominent absorption either around 480 nm (*anti*) or around 550 nm (*syn*). There is no such band in the experimental spectrum shown in

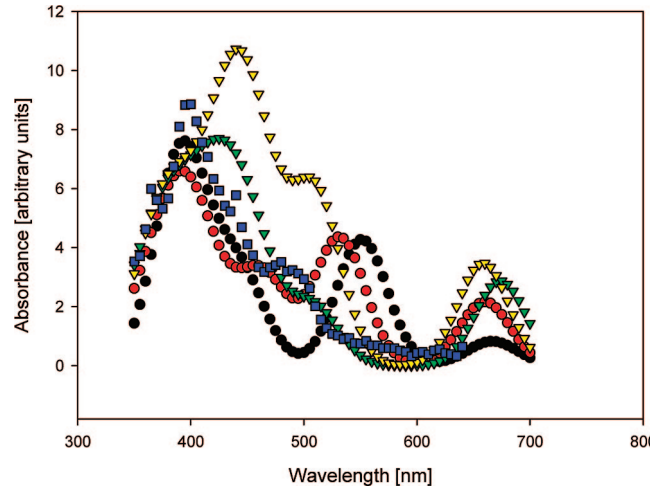

FIGURE 4. Comparison of the experimental transient spectrum of the short-lived intermediate (see also Figure 1) observed upon 355 nm LFP of **1b′** (blue) with the calculated UV/vis spectra of triplet-state stereoisomers of **1B′**. Black: *syn-E*-**1B′** triplet II. Red: *syn-Z*-**1B′** triplet II. Green: *anti-E*-**1B′** triplet II. Yellow: *anti-Z*-**1B′** triplet II. Blue: experimental spectrum (cf. Figure 1), scaled to match the calculated spectra in intensity.

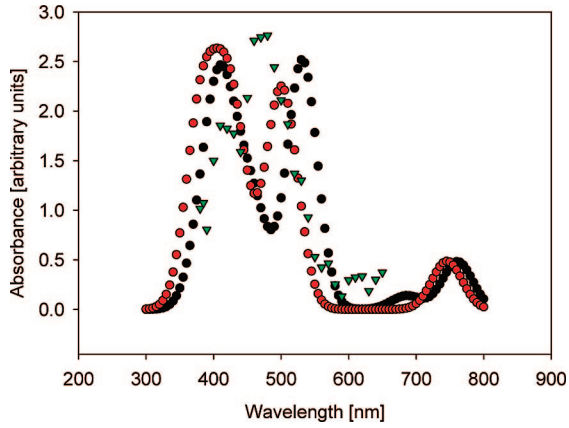

FIGURE 5. Comparison of calculated UV/vis-spectra (TD-UB3LYP/6-31+G*//UB3LYP/6-31G*) of the singlet and triplet states of **11B** with the experimental difference spectrum of the long-lived transient observed after LFP (355 nm) of **1b** in cyclohexane (cf. Figure S4, see the Supporting Information). Red: *Z*-**11B**-triplet. Black: *Z*-**11B**-singlet. Green: experimental transient difference spectrum, scaled to match the calculated spectra in intensity.

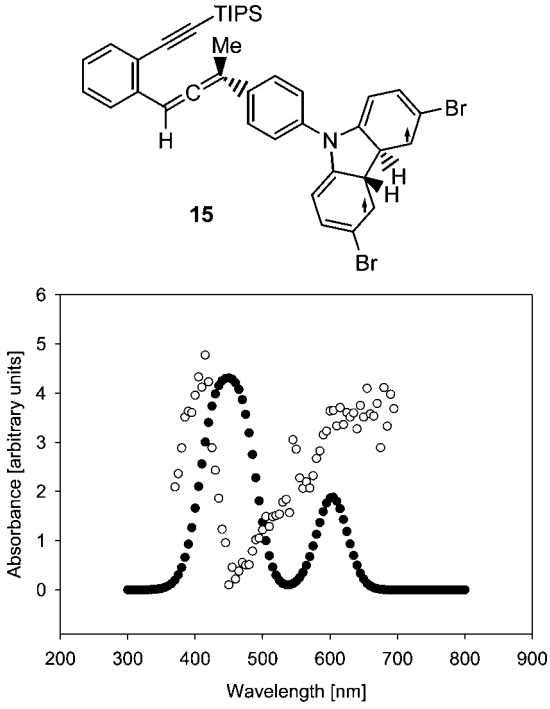

FIGURE 6. Comparison of calculated UV/vis spectra (TD-UB3LYP/6-31+G*//UB3LYP/6-31G*) of the first triplet excited-state of **15** with the experimental transient difference spectrum observed after LFP (266 nm) of **1b′** in cyclohexane (cf. Figure S7, Supporting Information). Black circles: Calculated spectrum of triplet **15**. Light circles: experimental transient spectrum, scaled to match the calculated spectra in intensity.

Figure 6. Third, the relative intensities at $\lambda = 400$ and 650 nm are very different in the calculated and experimental spectra.

To conclude this section, we may thus state that TD-DFT calculations give good support to the assignment of the short-lived transient observed upon LFP of **1b** and **1b′** (at 355 nm) to an allene-type triplet excited state. Furthermore, the good agreement of the calculated spectra of *anti*-**1B′** triplets II with the experimental spectrum of the short-lived transient observed upon LFP (355 nm) of **1b′** suggests the existence of the *anti*-triplet II conformers. While the lack of reactivity toward oxygen may argue against such an assignment, we note that certain ($\pi \rightarrow \pi^*$) triplet states of aromatic ketones have been reported to show reduced reactivity toward $^3O_2$. Thus, triplet ($\pi \rightarrow \pi^*$) 4-phenylbenzophenone, with a triplet energy of 60.8 kcal mol^{-1},[25] reacts with molecular oxygen with a rate constant $k_{O2} = 7.8 \times 10^7$ M^{-1} s^{-1}.[28c] This value is well below the upper limit of $k_{O2} \approx 5 \times 10^8$ M^{-1} s^{-1} determined for the reaction of the short-lived transient observed upon LFP (355 nm) of **1b′** with oxygen.

We also conclude that the spectrum of the short-lived transient observed upon LFP (266 nm) of **1b′** is not reproduced well by the calculations of the triplet state stereoisomers of **1B′** (see also Figure 6). This issue will be taken up again later in the manuscript.

Calculations: Reactivity of Triplet Allenes and Follow-Up Reactions. In order to understand the role of the allene triplet II state for the formation of **8b**,**b′** and **10b**,**b′** via the putative intermediates **11b**,**b′**, we have also done extensive computations on the follow-up reactions of isomers *E*-**1B**,**B′**-triplet II and *Z*-**1B**,**B′**-triplet II. In all cases, formation of the fulvene-diyl type diradicals should occur from the *syn*- isomers of the **1B**,**B′**-triplet II, since the vinyl-type radical is in a good position to add to the triple bond of the alkyne moiety. *Syn-E*-**1B**-triplet II is expected to yield the fulvene diyl *E*-**11B**, in either the triplet or singlet spin state, while isomer *syn-Z*-**1B**-triplet II should yield fulvene diyl *Z*-**11B**, again either as singlet or as triplet species. Diradical *Z*-**11B** in its singlet spin manifold should further undergo ring closure to the Diels−Alder product **12B**, which is a well-known precursor[24] to **10B** (equivalent to **10b**), while *E*-**11B** is set to undergo a 1,5-hydrogen shift to yield the ene-product **8B**. Analogous reactions can be formulated for precursor **1B′** (Scheme 11). Scheme 11 does not include the *anti*-conformers of the allene-type triplet states. A similar scheme for **1B′**, calculated at the BLYP/6-31G(d) level of theory gives results that are very similar to the B3LYP results (see the Supporting Information, Scheme S1).

In cyclohexenyne−allene **1B**, the *syn-E*-conformer of the precursor triplet II excited-state is predicted to be exceedingly short lived, with a calculated activation enthalpy for ring-closure to the *E*-fulvene diyl triplet diradical of only 2.9 kcal mol^{-1}. The singlet state of *E*-**11B** is predicted to be slightly higher in energy than the triplet state ($\Delta H_{S-T} = 1.8$ kcal mol^{-1}). A transition state for the hydrogen transfer reaction yielding fulvene **8B** could be located, but the activation enthalpy is very small. If a spin-projection correction is employed, it disappears completely. Given the very small barrier for formation of *E*-**11B** and the negligible barrier for its decay, it appears highly unlikely that any intermediate along the route from *syn-E*-**1b** triplet to the fulvene product **8b** should be detectable in our experiments. The cyclization of *syn-Z*-**1B**-triplet II, on the other hand, is predicted to be hindered by an activation enthalpy. As before in the *E*-manifold, the singlet state of diradical *Z*-**11B** is foreseen to be higher in energy than the triplet state ($\Delta H_{S-T} = 3.5$ kcal mol^{-1}). From the singlet diradical, cyclization to **12B** can occur with a calculated activation enthalpy of $\Delta H^{\ddagger} = 5.3$ kcal mol^{-1}. Interconversion of *E*- and *Z*-**11B** diradicals should be relatively facile on the singlet hypersurface, with activation enthalpies $\Delta H^{\ddagger} = 6.4$ kcal mol^{-1} from the energetically lower-lying *E*-conformer and $\Delta H^{\ddagger} = 4.8$ kcal mol^{-1} from the *Z*-conformer, while the barrier is predicted to be higher on the triplet hypersurface ($\Delta H^{\ddagger} = 9.1$ kcal mol^{-1}). Detectable intermediates in our experiments are thus possibly the fulvenediyls *Z*-**11b**.

SCHEME 11. Reactions of Enyne−allene Triplet States with Calculated Reaction Enthalpies and Activation Enthalpies ((U)B3LYP/6-31G(d)). Energies (in kcal mol^{-1}) Relative to the *Z-syn* Precursor Allene-Type Triplet II (Upper Numbers Refer to the Cyclohexenyne−Allene 1B; Bottom Numbers (Underlined) Refer to the Benzene Derivative 1B′)

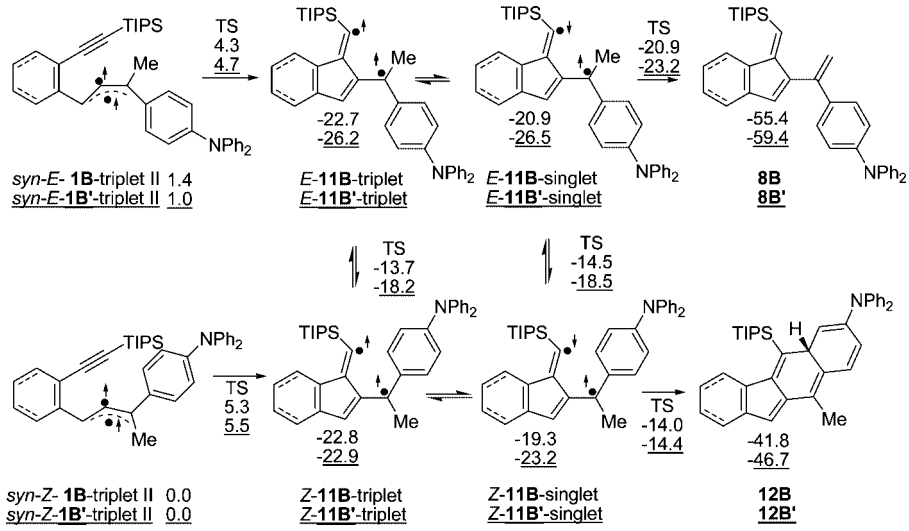

In case of **1B′**, the energetically lower-lying *syn-Z*-**1B′**-triplet II is predicted to show a somewhat higher barrier ($\Delta H^{\ddagger} = 5.5$ kcal mol^{-1}) toward addition to the alkyne C≡C bond, as compared to the *E*-isomer *syn-E*-**1B′**-triplet II ($\Delta H^{\ddagger} = 3.7$ kcal mol^{-1}). In this system, the singlet- and triplet-fulvenediyl-type diradicals are practically degenerate in energy. Hence, irrespective of the spin manifold, the barrier for interconversion of the *Z*- and *E*-diradicals is calculated as $\Delta H^{\ddagger} = 8.0$ kcal mol^{-1} from the energetically lower-lying *E*-conformer and $\Delta H^{\ddagger} = 4.7$ kcal mol^{-1} from the *Z*-conformer. The activation enthalpies for the follow-up reactions of the singlet diradicals parallel those predicted for system **1B**; cyclization of *Z*-**11B′** yielding **12B′** is predicted to be much slower ($\Delta H^{\ddagger} = 8.8$ kcal mol^{-1}) than H-transfer from *E*-**11B′** yielding **8B′** ($\Delta H^{\ddagger} = 3.3$ kcal mol^{-1}). According to the calculations, the preferred reaction path upon triplet excitation of **1B′** would thus involve formation of *syn-Z*-**1B′**-triplet II, followed by intramolecular addition to the C≡C triple bond yielding *Z*-**11B′** with nearly degenerate triplet and singlet states. Diradical *Z*-**11B′** is expected to relax to the more favorable *E*-**11B′**. Due to the small barrier for H-transfer *E*-**11B′** (and thus likely also *E*-**11b′**) should be only present in quasistationary concentrations. Detectable intermediates in our experiments are thus only *anti*-conformers of **1b′**-triplet II and *Z*-**11b′**.

It is interesting to note that the DFT results also agree in a qualitative manner with the experimental ene to Diels−Alder product ratios and their temperature dependence. The kinetically controlled product **8b,b′: 10b,b′** ratio should be related to the barriers of the rate determining steps, i.e., that of *Z*-**11B,B′** singlet → *E*-**11B,B′** singlet versus that of *Z*-**11B,B′** singlet → **12B,B′**. Indeed, for **11B** the computed barriers (4.8 vs. 5.3 kcal mol^{-1}) are almost identical (expt: **8b**:**10b** = 1:1), while for **11B′** the computed barrier of the Diels−Alder product formation is significantly higher by 4.1 kcal mol^{-1} (expt: **8b′**:**10b′** = ca. 2:1). Equally, the temperature dependence of the ene to Diels−Alder product ratio **8b′**:**10b′** is reproduced by the computations. The increasing amount of ene product **8b′** formed at higher temperature is due to a positive activation entropy of the *Z*-**11B′** singlet → *E*-**11B′** singlet reaction and a negative activation entropy of the *Z*-**11B′** singlet → **12B′** step (see Table S1, Supporting Information).

Assignment of the Long-Lived Transient in the Photolysis of 1b and 1b′ (266 nm). Our calculations suggest that the short-lived species observed in the experiments with **1b** ought to be an *anti*-conformer of an allene-type triplet II excited state of **1b**, while the long-lived transient would be either the singlet or the triplet state of *Z*-**11b**. Using the calculated reactivity data, the long-lived transient can be assigned to triplet *Z*-**11b** because its effective barrier to **12b**, consisting of the S-T energy gap and the barrier for ring closure, would be of the order of 9 kcal mol^{-1}, in agreement with a lifetime of 33 μs. Assigning this transient to triplet *Z*-**11b**, however, holds the problem that a triplet diradical would be expected to react rapidly with oxygen. In order to address the issue of spin multiplicity of the diradical observed, we have performed a series of calculations (UB3LYP/cc-pVTZ and UBLYP/cc-pVTZ) on fulvene diyl diradicals **13** bearing a variety of substituents (R = F, Cl, Br, H, Me, H_3Si, Li) and compared those with calculations on *Z*-**11B**.

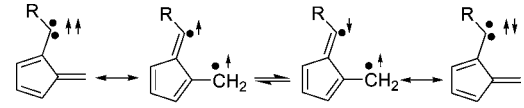

R = F, Cl, Br, CH_3, SiH_3, Li

The fact, that carbene-type mesomeric structures exist[11] is of particular relevance, for it implies that rules pertaining to singlet−triplet energy gaps in carbenes might also apply. Table 5 gives the calculated singlet - triplet energy gaps along with the important angle around the carbenic carbon atom. The data clearly indicate that the fulvene diyls investigated here follow the rules accepted for carbenes.[29a] σ-Acceptor substituents like the halogen atoms result in stabilization of the singlet spin manifold, while electron-donating substituents stabilize the triplet. The angles around the "carbenic" carbon atom also follow the trend observed for carbenes, with small angles for ground-state singlets and larger angles for ground-state triplet species. The data in Table 5 also show that B3LYP, in comparison to BLYP, places the triplets lower in energy. The preference for the triplet state is calculated to be smaller in *Z*-**11B** than in the model diradicals. Nevertheless, both functionals employed yield a triplet ground-state for *Z*-**11B**.

TABLE 5. Singlet−Triplet Energy Gap for Fulvene Diyls, As Calculated at the UB3LYP/cc-pVTZ or UBLYP/cc-pVTZ Levels of Theory, Except for *Z*-11B (6-31G(d)-Basis) (The Singlet Energies Have Been Corrected for Spin Projection Error. Positive Singlet−Triplet Energy Gaps Imply a Triplet Ground State. Angle around the "Carbene" Atom (UBLYP))

R, compd **13**	$\Delta H_{(S-T)}$ (kcal mol^{-1}) B3LYP (BLYP)	angle around "carbene" carbon (deg) (BLYP)
H	singlet not converged (+4.0)	S: 139.1 T: 138.5
F	−6.7 (−8.0)	S: 107.8 T: 128.7
Cl	−1.3 (−2.5)	S: 111.9 T: 134.0
Br	−0.8 (−2.4)	S: 112.5 T: 134.4
CH_3	singlet not converged (+7.7)	S: 124.2 T: 141.6
SiH_3	+17.8 (+9.6)	S: 145.4 T: 165.9
Li	+32.4 (+18.2)	S: 178.7 T: 178.9
Z-**11B**	+3.5 (+1.2)	S: 166.3 T: 165.2

SCHEME 12. Calculated Activation and Reaction Enthalpy for the Reaction of Model Diradical *Z*-11*β* with Oxygen

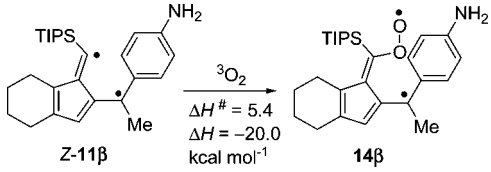

Our data suggest that triplet-**11B** (and thus triplet-**11b**) may be compared to triplet carbenes that bear very space-demanding substituents. Less than diffusion-controlled reactivity toward molecular oxygen has frequently been observed for such species. Didurylcarbene, which is significantly less shielded than **11B**, reacts with oxygen only at a fraction of the diffusion controlled rate limit ($k_{O2} = 4.1 \times 10^7$ M^{-1} s^{-1}).[29b] Triplet di-9-anthrylcarbene has been reported to react with oxygen with a rate constant $k_{O2} \approx 5 \times 10^5$ M^{-1} s^{-1}.[30] Hence, the absence of reactivity toward oxygen does not rule out a triplet ground-state for **11b**.

Calculating the barrier for the reaction of a triplet diradical like *Z*-**11B** with triplet molecular oxygen is difficult. In order to reduce the computational cost we have studied this reaction for a simplified model compound, triplet *Z*-**11*β*** (Scheme 12), which is oxidized to the peroxy-diradical **14*β***. Including a spin projection correction for the singlet transition state, the activation enthalpy obtained by UB3LYP/6-31G(d) is 5.4 kcal mol^{-1}.[31] We note that the singlet peroxydiradical **14*β*** that would initially be formed in this reaction is predicted to have a closed-shell ground state ($S^2 = 0$).

The reason for a barrier of 5.4 kcal mol^{-1} likely lies in the steric shielding of the reactive center, which is positioned in a deep pocket provided by the triisopropylsilyl group and the aniline moiety. Given the rather low concentration of oxygen in oxygen-saturated cyclohexane ($[O_2]_{sat} = 11.5$ mmol),[26] even this very modest activation barrier would be sufficient to prevent reaction of *Z*-**11*β***, and thus likely also *Z*-**11b**, with oxygen.

Time-dependent DFT was also employed to aid in the spectral assignment of the long-lived transients in the photochemistry of **1b**. Figure 5 shows a comparison of the calculated spectra of the singlet and triplet states of *Z*-**11B** with the experimental difference spectrum of the slowly decaying transient observed upon LFP of **1b**. While the essential features of the experimental spectrum (double band with $\lambda = 410$, 480 nm in the visible range of the spectrum) in principle are in agreement with the calculated spectra, the relative intensities of the two bands and their spacing are not reproduced well. The comparison does not allow for a conclusive assignment of the spin state of the diradical observed. It must be noted, however, that the experimental spectrum shown in green in fact is a transient difference spectrum (cf. Figure S4, see the Supporting Information). Any absorption of a product formed concomitantly with the decay of *Z*-**11b** would change relative intensities or shift maxima.

The long-lived transient observed upon LFP (266 nm) of **1b′** has a UV/vis-spectrum (see Figure S6, Supporting Information) that is very similar to the spectrum of the long-lived transient observed upon LFP of **1b** (Figure S4, Supporting Information). For that reason, it appears very likely that this species can be assigned to a fulvene diyl-type diradical. Our calculations indicate that this should be *Z*-**11b′**, as the *E*-conformer should be too short-lived for detection. Again, the spin multiplicity cannot be derived by comparing calculated vs. experimental spectra, as the spectra of the singlet and triplet states of *Z*-**11B′** are predicted to be very similar (Figure S10, see the Supporting Information).

While we have been able to identify some of the transient species with confidence, a number of open questions remain at this point.

Assignment of the Short-Lived Transient of 1b′ after Excitation at 266 nm. Experimental evidence suggests an analogy between the photochemical behavior of **1b** and the photoreactivity of **1b′** upon 266 nm excitation. However, the agreement between the experimental transient UV/vis-spectrum (see Figure S7 (Supporting Information) and the experimental spectrum shown in Figure 6) and the calculated spectrum of any of the stereoisomers of triplet **1B′** (cf. Figure S10, Supporting Information) is poor.

In order to address this point of concern, we need to discuss some alternative mechanistic pathways that are known to be of importance in photochemical transformations of allenes and triarylamines. Di- and triphenylamine have been reported to undergo a photochemical cyclization to carbazole derivatives *via* dihydrocarbazole diradicals.[32] The triplet energy of triphenylamine[26,33] has been reported as 69.6 kcal mol^{-1}, which is far higher than the triplet energies of the precursors investigated in this work. As a consequence, the spin density in the triphenylamine moiety is predicted to be small for the first triplet states of **1B** and **1B′**, and any carbazole-forming reaction starting from the lowest excited triplet state of **1b′** would be expected to have a very low quantum yield for that reason. Our product studies gave no evidence for carbazole-derived products. Also, the characteristic and intense absorption of the rather long-lived singlet dihydrocarbazole diradical at $\lambda = 610 - 620$[32a] nm was not observed in our experiments. On the other hand, in our experiments employing 266 nm excitation, higher excited precursor states may play a role, which might

(29) (a) Nemirowski, A.; Schreiner, P. R. *J. Org. Chem.* **2007**, *72*, 9533–40. (b) Tomioka, H.; Okada, H.; Watanabe, T.; Banno, K.; Komatsu, K.; Hirai, K. *J. Am. Chem. Soc.* **1997**, *119*, 1582–1593.

(30) Astles, D. J.; Girard, M.; Griller, D.; Kolt, R. J.; Wayner, D. D. M. *J. Org. Chem.* **1988**, *53*, 6053–6057.

(31) Oxygen attack at other positions is less favorable.

(32) (a) Suzuki, T.; Kajii, Y.; Shibuya, K.; Obi, K. *Bull. Chem. Soc. Jpn.* **1992**, *65*, 1084–1088. (b) Chattopadhyay, N.; Serpa, C.; Purkayastha, P.; Arnaut, L. G.; Formosinho, S. J. *Phys. Chem. Chem. Phys.* **2001**, *3*, 70–73. (c) Förster, E. W.; Grellmann, K. H. *Chem. Phys. Lett.* **1972**, *14*, 536–538. (d) Compared to the experimental system, only the *n*-butyl group has been replaced by a methyl group in **15**. An alternative dihydrocarbazole triplet **15b**, where the ring closure reaction involves the benzene ring connected to the allene moiety, is calculated to be higher in energy than **15**.

(33) McGlynn, S. P.; Azumi, T.; Kinoshita, M. *Molecular Spectroscopy of the Triplet State*; Prentice Hall: Englewood Cliffs, NJ, 1969.

open up channels not available from the lowest excited precursor singlet states. A comparison of the experimental transient UV/vis spectrum of the short-lived transient observed upon 266 nm LFP of **1b′** with the calculated UV/vis spectrum of a model dihydrocarbazole triplet excited state **15**[32c] reveals a general agreement in the spectral pattern (Figure 6). Hence a dihydrocarbazole triplet, likely accessible only from an upper singlet excited-state only populated upon 266 nm excitation, may indeed play the role of internal triplet sensitizer. In agreement with the rather weak transient intensities monitored upon 266 nm LFP of **1b′**, the calculated oscillator strengths of the transitions of triplet **15** are also smaller than the oscillator strengths of transitions of allene-type triplet II states of **1b′**. Given this agreement, a tentative assignment of the short-lived transient observed upon 266 nm, excitation of **1b′** to a dihydrocarbazole triplet state appears justified.

Long-Lived Transient Received after Excitation of 1b′ at 355 nm. The second open question relates to the nature of the long-lived transient observed upon 355-nm excitation of **1b′**, which has not yet been identified. Given the fact that two minor unidentified products are formed if a preparative irradiation of **1b′** is performed at $\lambda_{exc} = 350$ nm, it appears plausible that the transient observed in the LFP experiment and the unidentified trace products are linked to each other.

Arylallenes, if irradiated in the absence of external quenchers, have been reported to undergo hydrogen- or aryl-shift reactions resulting in the formation of carbene-derived products.[34] Thus, irradiation of triphenylallene in degassed cyclohexane yields diphenylindenes, whose formation can be rationalized by intramolecular addition of a phenylvinyl carbene to one of the benzene rings.[34] This reaction occurs rather inefficiently in the photochemistry of triphenylallene.[34] The formation of two minor unidentified products upon long-wavelength excitation of **1b′** therefore could be related to photochemical phenylvinylcarbene formation. Triplet phenylvinylcarbenes thus remain a possible, but as yet unproven assignment for the long-lived transient observed upon 355 nm excitation of **1b′**.

Formation of the *syn*-Enyne−Allene Triplets. According to our product studies and LFP experiments, C^2-C^6 cyclization does occur upon excitation of allenes **1b** and **1b′**. This reaction requires the formation of *syn*-conformers of allene-type triplet states of the two precursors. Observation of Stern−Volmer quenching of diradical *Z*-**11b** upon addition of oxygen indicates that at least a significant portion of *Z*-**11b** must be formed *via* an observable triplet state of **1b** with a lifetime $\tau \sim 58$ ns, which is in qualitative agreement with the value measured directly for the short-lived transient in this system. As a consequence, we would have to postulate that at least a significant portion of the allene triplet state formed upon excitation of **1b** must be in a *syn*-conformation. The latter, i.e., triplet *syn*-^{3}**1b**, is formed either directly from ground state *syn*-**1b** or via facile bond rotation from triplet *anti*-^{3}**1b**. In contrast to the DFT results, our RIMP2 calculations indeed predict that the *syn*-conformers of ground state **1B** and **1B′** should be favored by 0.9 and 2.9 kcal mol^{-1}, respectively, relative to the *anti*-conformers. Equilibrium ratios can thus be estimated as *anti*-/*syn*-**1b** = 22:78 and as *anti*-**1b′**/*syn*-**1b′** = 0.7:99.3. If the conclusion from the RIMP2 calculations holds that the *syn* conformers should be preferred, the experimental observations are therefore easily rationalized.

On the other hand, an alternative mechanistic scenario involving a bond rotation of the primarily formed *anti*-conformers on the triplet hypersurface into *syn*-conformers is highly unlikely given the calculated barriers of 9 − 12 kcal mol^{-1} (cf. Schemes 9 and 10). Such barriers cannot be reconciled with the observed very short triplet lifetimes.

Effect of Benzannulation. What is the effect of benzannulation on the photochemical C^2-C^6 cyclization of enyne−allenes? Our data indicate that the impact of benzannulation is quite small as far as the mechanism, thermodynamics and kinetics of the cyclization reaction itself are concerned. Equally, an evaluation of the yields (see Table 2) obtained in the preparative photolyses does not show vast differences, although the yields are consistently a little bit higher for all benzannulated representatives. The most notable difference is thus the wavelength dependence seen in the LFP study, suggesting that the observed discrepancies arise from different competing excited states. For simple enyne−allenes, for example, twisted-alkene type triplet states (triplet I) are almost degenerate in energy with the lowest allene-type triplet (triplet II) states, while for benzannulated enyne−allenes only the triplet II states matter. Moreover, the degree of Franck−Condon overlap between singlet and triplet excited states may be a factor that is crucial in determining ISC efficiency and also the type of triplet state being formed. Additional flexibility in accommodating triplet energy, such as it is available to **1b** (but not **1b′**) in form of the triplet I state, will certainly help in this respect. The formation of a dihydrocarbazole-type triplet state of rather high energy upon 266 nm; LFP of **1b′** might find its explanation along these lines. However, since no photophysical study was conducted, an in-depth discussion of the role of the triplet I and possibly competing singlet excited states certainly is premature at the present stage.

Conclusions

The results obtained from product, LFP, and DFT studies on the photochemical C^2-C^6 cyclization of benzannulated and nonbenzannulated enyne−allenes now provide a conclusive picture. Accordingly, the photochemical reaction sequence involves the excitation of the *syn*-enyne−allene to a highly reactive *syn*-enyne−allene triplet II species. Due to its rapid follow-up cyclization ($\Delta H^{\ddagger} = 4-5$ kcal mol^{-1}) to a triplet fulvene diyl, the *syn*-enyne−allene triplet is not visible in the LFP experiment. Rather, the unproductive *anti*-enyne−allene triplet, not likely to undergo a energetically demanding bond rotation during its short lifetime, was assigned to the short-lived transient. The long-lived transient was assigned to the triplet fulvene diyl based on the good agreement of experimental data (spectra, product ratios) and DFT results. This intermediate, generated in two conformations (*E* and *Z*), will afford the observed products after a triplet to singlet interconversion. The thus derived reaction mechanism, exhaustively evaluated by DFT, is in full agreement with experimental data, such as product ratio and its temperature dependence.

A DFT investigation on a series of fulvene diyls bearing a variety of substituents indicates substituent effects on the singlet−triplet energy gap that are similar to the effects generally observed in the case of carbenes. The calculations indicate a slight preference of triplet *E*-**11B** and *Z*-**11B** over the singlet state of these diradicals, whereas the singlet and triplet states are predicted to be almost degenerate for the benzannulated derivatives *E*-**11B′** and *Z*-**11B′**.

(34) Klett, M. W.; Johnson, R. P. *J. Am. Chem. Soc.* **1985**, *107*, 3963–3971.

Experimental Section

The photochemical reactions of enyne−allene **1a**−**1c** and **1a′**−**c′** were performed under nitrogen atmosphere, using a Rayonet RPR-100 Photochemical reactor (16 lamps) at 300 nm wavelength in dry degassed toluene/*n*-hexane (at 17 ± 2 °C).

Laser Flash Photolysis. The system employed has already been described.[35] The precursor allenes were excited using the third harmonic (λ = 355 nm) or fourth harmonic (λ = 266 nm) of a Nd:YAG laser (Quanta-Ray Laboratory 130, 120 mJ/pulse (third harmonic), 50 mJ/pulse (fourth harmonic), 7 ns pulse duration). The precursor concentrations were adjusted to an optical density OD = 0.3 at the laser wavelength. A flow cell was used in order to avoid buildup of photoproducts. Prior to experiments, the solutions were purged with argon for ca. 20 min. The cyclohexane used in the experiments was of spectroscopic grade.

Computational. The program package Gaussian 03[36] was used for the DFT calculations. All calculated minima and transition states were characterized as such by performing a vibrational analysis. All calculated reaction and activation enthalpies include a zero point vibrational energy correction. The energies of singlet diradicals and transition states of singlet diradical reactions were corrected by performing a spin projection correction.[37] We used the pure density functional BLYP[38] and the hybrid B3LYP[38] method in combination with 6-31G(d) or 6-31+G(d)[39] and cc-pVTZ[40] basis sets. UV/vis spectra were calculated using time-dependent B3LYP/6-31+G(d)[41] based on B3LYP/6-31G(d) geometries. RIMP2 single-point energy calculations[42] with a TZVP[43] basis set were performed using Turbomole software.[44] The UV/vis spectra shown were generated from the calculated transition intensities and positions by overlaying a Gaussian function over each transition (program kindly provided by Koop Lammertsma).

{2-[3-(4-Bromonaphthalen-1-yl)hepta-1,2-dienyl]phenylethynyl}triisopropylsilane (1a′). To a solution of 1,4-dibromonaphthalene (1.53 g, 5.36 mmol) in dry diethyl ether (60 mL), cooled to 0 °C by an ice bath, was added *n*-BuLi (2.5 M, 2.14 mL, 5.36 mmol) dropwise. After being stirred for 4 h, the reaction mixture was added dropwise to 1 M $ZnCl_2$ solution (731 mg in 5.4 mL of diethyl ether) and stirred for 30 min at room temperature. After the reaction mixture was cooled to −60 °C, $Pd(PPh_3)_4$ (155 mg, 134 μmol) in dry THF (5 mL) was added dropwise, and after the mixture was stirred for 30 min at the same temperature, propargyl acetate **5′** (550 mg, 1.34 mmol) in dry THF (10 mL) was added dropwise. After being stirred for 16 h at room temperature, the reaction mixture was quenched with aqueous saturated ammonium chloride solution. The aqueous layer was washed with pentane (2 × 100 mL). The combined organic layer was dried over sodium sulfate and evaporated under reduced pressure. After purification by column chromatography (silica gel, *n*-pentane, R_f = 0.53) compound **1a′** was isolated as colorless oil: yield 220 mg, 30%; IR (film) ν 3051 (w), 2943 (s, C−H), 2865 (s), 2253 (s), 2151 (s), 1943 (m), 1583 (w), 1504 (m), 1484 (m), 1465 (s), 1376 (s), 1265 (s), 1091 (m), 996 (m), 909 (s), 832 (m), 734 (s), 651 (s), 546 (w) cm^{-1}; ^1H NMR (400 MHz, $CDCl_3$) δ 0.91 (t, ^3J = 7.3 Hz, 3H), 1.16 (s, 21H), 1.43 (sextet, ^3J = 7.3 Hz, 2H), 1.52−1.62 (m, 2H), 2.52−2.67 (m, 2H), 6.99 (t, ^5J = 3.0 Hz, 1H), 7.13 (td, $^{3,4}J$ = 7.6 and 1.2 Hz, 1H), 7.28 (td, $^{3,4}J$ = 7.6 and 1.2 Hz, 1H), 7.35 (d, ^3J = 7.6 Hz, 1H), 7.45 (dd, $^{3,4}J$ = 7.6 and 1.2 Hz, 1H), 7.53−7.63 (m, 3H), 7.77 (d, ^3J = 7.6 Hz, 1H), 8.22 (dd, $^{3,4}J$ = 8.2 and 1.0 Hz, 1H), 8.28 (dd, $^{3,4}J$ = 8.2 and 1.0 Hz, 1H); ^{13}C NMR (100 MHz, $CDCl_3$) δ 11.3, 13.9, 18.7, 22.5, 30.1, 34.6, 93.5, 95.7, 105.0, 107.7, 121.4, 122.2, 125.9, 126.0, 126.3, 126.5, 126.8, 127.2, 127.7, 128.5, 129.5, 132.3, 132.6, 132.9, 136.1, 136.6, 205.3 ppm; MS-EI (70 eV) *m/z* 556.2 (0.2, M^+); HRMS calcd for $C_{34}H_{41}BrSi$ 556.216, found 556.216.

Bis(4-bromophenyl)-[4-(1-{2-[(triisopropylsilanyl)ethynyl]phenylvinylidene}pentyl]phenyl]amine (1b′). In 30 mL of dry diethyl ether tris-(*p*-bromophenyl)amine (1.41 g, 2.92 mmol) was cooled to 0 °C in an ice bath. *n*-BuLi (2.5 M) (1.17 mL, 2.92 mmol) was added dropwise and stirred. After 4 h, this reaction mixture was added dropwise to a 1 M $ZnCl_2$ solution (398 mg in 2.92 mL of diethyl ether) and stirred for 60 min at room temperature. The reaction mixture was then cooled to −60 °C, and $Pd(PPh_3)_4$ (84.0 mg, 72.7 μmol) in dry THF (5 mL) was added dropwise. After the mixture was stirred for 30 min at the same temperature, propargyl acetate **5′** (300 mg, 0.73 mmol) in dry THF (10 mL) was added dropwise. After being stirred for 16 h at room temperature, the reaction mixture was quenched with aqueous saturated ammonium chloride solution. The aqueous layer was washed with pentane (2 × 50 mL). The combined organic layers were dried over sodium sulfate and evaporated under reduced pressure. After purification by column chromatography (silica gel, *n*-pentane, R_f = 0.58) compound **1b′** was isolated as light yellow oil: yield 265 mg, 48%; IR (NaCl) ν 3053 (s), 2987 (m), 2865 (w), 2685 (w), 2151 (w), 1923 (w), 1581 (w), 1486 (m), 1421 (m), 1313 (w), 1265 (s), 1072 (w), 1007 (w), 896 (s), 824 (w), 739 (s) cm^{-1}; ^1H NMR (400 MHz, acetone-d_6) δ 0.91 (t, ^3J = 7.3 Hz, 3H), 1.17 (brs, 21H), 1.40−1.50 (m, 2H), 1.55−1.64 (m, 2H), 2.52−2.67 (m, 2H), 6.98 (d, ^3J = 9.1 Hz, 4H), 7.05 (d, ^3J = 8.8 Hz, 2H), 7.20 (t, ^5J = 2.9 Hz, 1H), 7.22 (td, $^{3,4}J$ = 7.5 and 1.3 Hz, 1H), 7.33 (td, $^{3,4}J$ = 7.8 and 1.3 Hz, 1H), 7.42 (d, ^3J = 8.8 Hz, 2H), 7.43 (d, ^3J = 9.1 Hz, 4H), 7.49 (dd, $^{3,4}J$ = 7.5 and 1.1 Hz, 1H), 7.51 (td, $^{3,4}J$ = 7.8 and 1.1 Hz, 1H); ^{13}C NMR (100 MHz, acetone-d_6): δ 11.9, 14.2, 19.0, 23.1, 30.3, 30.8, 96.1, 96.6, 106.1, 110.6, 116.0, 121.9, 125.4, 126.5, 126.9, 127.9, 128.2, 129.9, 131.8, 133.3, 133.8, 137.3, 146.8, 147.4, 208.1 ppm; MS-EI (70 eV) *m/z* 751.2 $[M]^+$; HRMS calcd for $C_{42}H_{47}Br_2NSi$ 751.184, found 751.184.

3-Ethyl-5-{2-[triisopropylsilylethynyl]phenyl}penta-3,4-dien-2-one (1c′). A mixture of LDA (2.33 mmol) and HMPA (0.41 mL, 2.33 mmol) in THF (30 mL) was treated at −80 °C dropwise with a solution of **7′** (550 mg, 1.94 mmol) in 15 mL of THF. After the mixture was stirred for 40 min at the same temperature, a solution of 2-bromo-3-pentanone (476 mg, 2.92 mmol) in THF (10 mL) was added dropwise. After 30 min, the reaction mixture was allowed to warm to room temperature and quenched with water (40 mL). The aqueous layer was extracted with diethyl ether (2 × 50 mL). The combined layers were dried over sodium sulfate and concentrated under reduced pressure. After purification by column chromatography (silica gel, *n*-hexane, R_f = 0.70 *n*-pentane/diethyl ether 9:1) **1c′** was isolated as yellow oil: yield 230 mg, 32%; IR (film) ν 2944 (m, C−H), 2866 (m), 2254 (m), 2152 (m), 1933 (m), 1677 (s), 1461 (m), 1360 (w), 1265 (s), 1238 (m), 997 (w), 908 (s), 850 (w), 734 (s), 651 (m) cm^{-1}; ^1H NMR (200 MHz, $CDCl_3$) δ 1.07 (t, ^3J = 7.3 Hz, 3H), 1.17 (s, 21H), 2.32 (s, 3H), 2.33−2.47 (m, 2H), 7.16−7.29 (m, 3H, Ar−H), 7.37 (td, $^{3,4}J$ = 7.5 and 1.5 Hz, 1H), 7.53 (dd, $^{3,4}J$ = 7.5 and 1.5 Hz, 1H); ^{13}C NMR (50 MHz, $CDCl_3$) δ 11.3, 12.3, 18.7, 20.3, 27.4, 96.6, 97.4, 104.5, 114.8, 121.9, 126.2, 127.4, 128.8, 133.1, 134.2, 198.0, 215.4 ppm; MS-EI (70 eV) *m/z* 366.2 $[M]^{+\cdot}$; HRMS calcd for $C_{24}H_{34}OSi$ 366.238, found 366.238.

{(1*E*)-(2-[(*E*)-1-(4-Bromonaphthalen-1-yl)pent-1-enyl]-1*H*-inden-1-ylidenemethyl}triisopropylsilane (8a′). In 10 mL of dry toluene, 36.0 mg (76.0 μmol) of enyne−allene **1a′** was refluxed for 40 h. After removal of toluene under reduced pressure and purification by chromatography (aluminum sheet, silica gel 60 F_{254}, *n*-pentane, R_f = 0.53), compound **8a′** was isolated as yellow oil: yield:33 mg, 91%; IR (film) ν 2945 (s), 2866 (s), 2253 (m), 1581

(35) Bucher, G. *Eur. J. Org. Chem.* **2001**, 2463–2475.
(36) Frisch, M. J. et al. *Gaussian03*; Gaussian, Inc.: Wallingford, CT, 2004.
(37) Goldstein, E.; Beno, B.; Houk, K. N. *J. Am. Chem. Soc.* **1996**, *118*, 6036–6043.
(38) Becke, A. D. *J. Chem. Phys.* **1993**, *98*, 5648–5652.
(39) Ditchfield, R.; Hehre, W. J.; Pople, J. A. *J. Chem. Phys.* **1971**, *54*, 724–728.
(40) Dunning, T. H., Jr. *J. Chem. Phys.* **1989**, *90*, 1007–1023.
(41) Bauernschmitt, R.; Ahlrichs, R. *Chem. Phys. Lett.* **1996**, *256*, 454–464.
(42) Weigend, F.; Häser, M. *Theor. Chem. Acc.* **1997**, *97*, 331–340.
(43) Weigend, F.; Ahlrichs, R. *Phys. Chem. Chem. Phys.* **2005**, *7*, 3297–3305.
(44) *TURBOMOLE V5-9-1*; University of Karlsruhe: Karlsruhe, 2007.

(w), 1504 (m), 1461 (m), 1379 (m), 1256 (w), 1199 (w), 1105 (w), 1015 (w), 908 (s), 832 (w), 734 (s), 651 (s), 577 (w) cm^{-1}; ^1H NMR (400 MHz, $CDCl_3$) δ 0.97 (t, ^3J = 7.3 Hz, 3H), 1.02 (d, ^3J = 7.4 Hz, 18H), 1.35 (septet, ^3J = 7.4 Hz, 3H), 1.54 (sextet, ^3J = 7.3 Hz, 2H), 2.32 (q, ^3J = 7.4 Hz, 2H), 6.08 (t, ^3J = 7.4 Hz, 1H), 6.56 (d, ^{5}J= 0.8 Hz, 1H), 6.67 (s, 1H), 7.12−7.17 (m, 2H), 7.21 (dd, $^{3,4}J$ =7.2 and 0.9 Hz, 1H), 7.25 (d, ^{3}J=7.7 Hz, 1H), 7.40−7.44 (m, 1H), 7.52−7.56 (m, 1H), 7.68 (d,^3J = 7.3 Hz, 1H), 7.71 (d, ^3J = 7.8 Hz, 1H), 8.25 (dd, ^3J = 8.3 and 0.6 Hz, 1H), 8.30 (d, ^3J = 8.6 Hz, 1H); ^{13}CNMR (100 MHz, $CDCl_3$) δ 12.9, 13.9, 19.0, 23.0, 32.9, 120.6, 121.7, 122.1, 124.8, 126.4, 126.6, 126.8 (2C), 127.4, 128.1, 129.3, 129.4, 131.1, 132.2, 132.3, 132.8, 133.4, 136.0, 137.7, 142.2, 143.8, 155.0 ppm; MS-EI (70 eV) *m/z* 556.2 $[M]^+$; HRMS calcd for $C_{34}H_{41}BrSi$ 556.216, found 556.216.

Bis(4-bromophenyl)-[4-((1*E*)-1-{3-[1-triisopropylsilanylmeth-(*E*)-ylidene]-3*H*-inden-1-yl)pent-1-enyl)phenyl]amine (8b′). In 15 mL of dry toluene, 30.0 mg (39.0 μmol) of enyne−allene **1b′** was refluxed for 5 h. After removal of toluene under reduced pressure and purification by chromatography (preparative TLC, silica gel 60 F_{254}, *n*-pentane, R_f = 0.35) compound **8b′** was isolated as yellow oil: yield 25 mg, 83%; IR (film) ν 2941 (s), 2863 (s), 1580 (m), 1505 (m), 1485 (s), 1312 (s), 1285 (m), 1072 (w), 1007 (w), 881 (w) cm^{-1}; ^1H NMR (400 MHz, C_6D_6) δ 0.82 (t, ^3J = 7.2 Hz, 3H), 1.04 (d, ^3J = 7.5 Hz, 18H), 1.31 (septet, ^3J = 7.5 Hz, 3H), 1.39 (sextet, ^3J = 7.3 Hz, 2H), 2.17 (q, ^3J = 7.3 Hz, 2H), 6.25 (t, ^3J = 7.4 Hz, 1H), 6.44 (d, ^5J = 0.8 Hz, 1H), 6.62 (d, ^3J = 8.8 Hz, 4H), 6.65 (s, 1 H), 6.81 (d, ^3J = 8.8 Hz, 2H), 7.08−7.14 (m, 7H), 7.28 (d,^3J = 8.6 Hz, 2H), 7.87 (dd, $^{3,4}J$ = 6.8 and 1.2 Hz, 1H); ^{13}CNMR (100 MHz, C_6D_6) δ 13.2, 13.9, 19.3, 23.3, 32.6, 115.7, 121.2, 122.5, 124.7, 125.2, 125.6, 127.9, 128.8, 131.3, 131.9, 132.2, 132.6, 135.8, 136.3, 138.5, 143.5, 144.7, 145.9, 146.7, 156.6 ppm; MS-EI (70 eV) *m/z* 751.2 (M^+); HRMS calcd for $C_{42}H_{47}Br_2NSi$ 751.184, found 751.184.

(3*Z*)-3-[(1*E*)-1-(Triisopropylsilylmethylene)-1*H*-inden-2-yl]pent-3-en-2-one (8c′). Enyne−allene **1c′** (46.0 mg, 0.12 mmol) was refluxed for 48 h in 15 mL of dry toluene. After removal of toluene under reduced pressure and purification by chromatography (preparative TLC: silica gel 60F_{254}, *n*-hexane/diethyl ether, 100:10, *n*-hexane/diethyl ether 9:1, R_f = 0.45) **8c′** was isolated as yellow oil: yield 37 mg, 80%; IR (film) ν 2943 (s), 2866 (s), 1690 (s), 1625 (m), 1462 (m), 1356 (m), 1265 (s), 881 (m), 740 (s), 704 (m), 659 (s) cm^{-1};^1H NMR (400 MHz, $CDCl_3$): δ 1.10 (d, ^3J = 7.5 Hz, 18H), 1.42 (septet, ^3J = 7.5 Hz, 3H), 1.72 (d, ^3J = 7.0 Hz, 3H), 2.19 (s, 3H), 6.13 (d, ^4J = 1.0. Hz, 1H), 6.69 (s, 1H), 7.14 (q, ^3J = 7.0 Hz, 1H), 7.16−7.20 (m, 1H), 7.24−7.29 (m, 2H), 7.72 (dd,$^{3,4}J$ = 7.4 and 0.7 Hz, 1H); ^{13}CNMR (100 MHz, $CDCl_3$) δ 12.9, 15.9, 19.1, 27.9, 120.8, 122.3, 125.1, 128.3, 131.2, 135.7, 137.6, 138.1, 139.6, 140.7, 143.8, 155.4, 198.5 ppm; MS-EI (70 eV) *m/z* 366.2 $[M]^+$; HRMS calcd for $C_{24}H_{34}OSi$ 366.238, found 366.238.

(5-Bromo-13-butyl-12*H*-indeno[1,2-*b*]phenanthren-7-yl) triisopropylsilane (9a′):^1H NMR (400 MHz, $CDCl_3$) δ 0.90 (t, ^3J = 7.2 Hz, 3H), 1.16 (s, 18H), 1.34−1.45 (m, 3H), 1.58−1.64 (m, 4H), 2.73 (t, ^3J = 7.9 Hz, 2H), 4.29 (s, 2H),7.34 (d, ^3J = 7.7 Hz, 1H), 7.65−7.73 (m, 2H), 7.79 (d, ^3J = 8.0 Hz, 1H), 7.90 (d, ^3J = 7.5 Hz, 1H), 7.96 (t, ^3J = 7.8 Hz, 2H), 8.35 (d, ^3J = 8.3 Hz, 1H); MS-EI (70 eV) *m/z* 556.2 (M^+); HRMS calcd for $C_{34}H_{41}BrSi$ 556.216, found 556.216.

Bis(4-bromophenyl)(10-butyl-11*H*-benzo[*b*]fluoren-7-yl)-amine (10): IR (film) ν 3054 (m), 2933 (m), 1580 (m), 1486 (m), 1262 (s), 1072 (m), 896 (m), 823 (m), 740 (s), 705 (s) cm^{-1}; ^1H NMR (400 MHz, $CDCl_3$) δ 1.00 (t, ^3J = 7.2 Hz, 3H), 1.54 (sextet, ^3J =7.3 Hz, 2H), 1.73 (quintet, ^3J = 7.7 Hz, 2H), 3.13 (t, ^3J = 7.9 Hz, 2H), 4.03 (s, 2H), 7.02 (d, ^3J = 8.9 Hz, 4H), 7.22 (dd, $^{3,4}J$ = 9.1 and 2.4 Hz, 1H), 7.32−7.40 (m, 2H), 7.37 (d, ^3J = 8.9 Hz, 4H), 7.52 (d, ^4J = 2.4 Hz, 1H), 7.56 (d, ^3J = 6.8 Hz, 1H), 7.83 (d, ^4J = 6.9 Hz, 1H), 7.87 (s, 1H), 7.96 (d, ^3J = 9.0 Hz, 1H); ^{13}C NMR (50 MHz, $CDCl_3$) δ 14.1, 23.3, 29.7, 32.4, 35.7, 115.5, 115.6, 120.6, 122.4, 123.4, 125.2, 125.3, 125.5, 126.9, 127.6, 128.3, 132.4, 134.5, 134.8, 138.6, 140.6, 141.4, 143.6, 143.7, 146.6 ppm; MS-EI (70 eV) *m/z* 595.05 (M^+); HRMS calcd for $C_{33}H_{27}Br_2N$ 595.051, found 595.051.

Acknowledgment. We are very much indebted to the Deutsche Forschungsgemeinschaft and the Fonds der Chemischen Industrie for continued support of our research.

Supporting Information Available: Experimental procedures for the preparation of and characterizations of **3**, **3′**, **4**, **4′**, **5**, **5′**, **6**, **6′**, **7**, and **7′**; ^1H and ^{13}C spectra of **1a′**−**c′**, **8a′**−**c′**, **9**, and **10′** and LFP results; UV−vis spectra of **1a′**−**c′**. Cartesian coordinates and energies of the stationary points optimized. This material is available free of charge via the Internet at http://pubs.acs.org.

JO801689W